

2

DOE/MC/26038-3823
(DE94012257)

**Facilitated Transport Ceramic Membranes for
High-Temperature Gas Cleanup**

**Final Report
February 1990 - April 1994**

**R. Quinn
E. Minford
A. S. Damle
S. K. Gangwal
B. A. Hart**

April 1994

Work Performed Under Interagency Agreement No.: DE-AC21-90MC26038

For
U.S. Department of Energy
Office of Fossil Energy
Morgantown Energy Technology Center
Morgantown, West Virginia

By
Air Products and Chemicals, Inc.
Allentown, Pennsylvania

MASTER

se

DISTRIBUTION OF THIS DOCUMENT IS UNLIMITED

**Facilitated Transport Ceramic Membranes for
High-Temperature Gas Cleanup**

**Final Report
February 1990 - April 1994**

**R. Quinn
E. Minford
A. S. Damle
S. K. Gangwal
B. A. Hart**

Work Performed Under Interagency Agreement No.: DE-AC21-90MC26038

**For
U.S. Department of Energy
Office of Fossil Energy
Morgantown Energy Technology Center
P.O. Box 880
Morgantown, West Virginia 26507-0880**

**By
Air Products and Chemicals, Inc.
7201 Hamilton Boulevard
Allentown, Pennsylvania 18195-1501**

April 1994

Table of Contents

	<u>Page</u>
List of Tables	iv
List of Figures	v
Executive Summary	vi
1.0 Background	1
2.0 Objectives and Project Description	5
2.1 Objectives	5
2.2 Project Description	5
3.0 Experimental Section	6
3.1 Salt Mixture Preparation and Characterization	6
3.1.1 Methods	6
3.1.2 Materials	6
3.2 Absorption Experiments	7
3.3 Membrane Preparation and Testing	13
3.3.1 Membrane Testing	13
3.3.2 Membrane Preparation	16
4.0 Results and Discussion	17
4.1 Development of Molten Carbonate Salts	17
4.1.1 Survey of H ₂ S Reactivity of Pure Carbonate Salts	17
4.1.2 Characterization of Pure Carbonate Salts	18
4.1.3 Preparation and Characterization of Carbonate Mixtures	26
4.1.4 Preparation and Characterization of Sulfide-Containing Carbonate Mixtures	30
4.1.5 Determination of Equilibrium Constants for the Reaction of H ₂ S with Molten Carbonate Mixtures	32
4.1.5.1 Gas Phase Reactivity	33
4.1.5.2 H ₂ S Absorption Experiments	34
4.1.5.3 H ₂ S-Metal Reactivity	36
4.2 Ceramic Materials Development	36
4.2.1 Materials Selection	37
4.2.2 Wetting Behavior	39
4.2.3 Ceramic Substrate Development	41
4.2.4 Ceramic Membrane Infiltration	45
4.3 Membrane Testing	49
4.3.1 Molten Carbonate/Gold Frit Membranes	50
4.3.2 Planar Molten Carbonate/Ceramic Membranes	51
4.3.2.1 Membrane Sealing	52
4.3.2.2 Testing with H ₂ S Containing Feeds	52
4.3.2.3 Testing with non-H ₂ S Containing Feeds	57
4.3.3 Alternative Materials of Construction for Membrane Cells	60
4.3.4 Planar and Tubular Molten Carbonate/Ceramic Membranes. Testing at RTI	61
4.3.5 Modeling of Membrane Performance	61

5.0	Summary and Conclusions	65
6.0	References	68
7.0	Appendix	70

List of Tables

Number		Page
3.1.1	Compositions and melting temperatures of carbonate mixtures prepared	6
4.1	Log K values for reactions 1-3 at 627°C for pure alkali and alkaline earth carbonates	18
4.2	Metal ion content of alkali and alkaline earth carbonates	20
4.3	High temperature weight losses for pure carbonate salts	24
4.4	Endotherms for pure metal carbonate salts between 30 and 100°C under a N ₂ atmosphere.	26
4.5	Compositions and melting temperatures of carbonate mixtures.	27
4.6	TGA results for carbonate salt mixtures. High temperature weight losses for mixtures under N ₂ or CO ₂ atmospheres	28
4.7	DTA results for carbonate mixtures. Observed endotherm temperatures between 30 and 1000°C for samples under N ₂ or CO ₂ atmospheres	30
4.8	DTA results for carbonate mixtures. Observed exotherm temperatures between 30 and 1000°C for samples under N ₂ or CO ₂ atmospheres	30
4.9	Composition of carbonate salt mixtures containing added sulfide ion.	31
4.10	DTA exotherm and endotherm temperatures for sulfide ion containing carbonate mixtures	32
4.11	Equilibrium constant values for gas phase reactions	34
4.12	Headspace analysis of gases at equilibrium in absorption experiment 12666-2	35
4.13	ESCA surface analysis of AlN samples	41
4.14	Capillary force as a function of support pore radius	44
4.15	Phase analysis of long term salt retention samples	45
4.16	Planar disc support infiltration results	48
4.17	Tubular support infiltration results	49
4.18	Calculated permeabilities of CO, CO ₂ , and H ₂ in a molten carbonate membrane.	50
4.19	Permselective properties of molten carbonate /gold frit membranes at 560°C	51
4.20	Listing of molten carbonate/ceramic planar membranes tested	52
4.21	Permselective properties of molten carbonate/ceramic membranes at 560°C using H ₂ S containing feeds	54
4.22	Elements present as determined by EDS in the membrane cell after evaluation of membrane 12496-2-3	55
4.23	Analysis of H ₂ S gas mixtures passed through a gold plated membrane cell at 560°C	55
4.24	Permselective properties of molten salt/ceramic membranes at 560°C using non-H ₂ S containing feeds	58
4.25	Permselective properties of molten carbonate/ceramic membranes at 560°C using non-H ₂ S containing feeds.	59
4.26	Analysis of 6% H ₂ S in N ₂ feed after passage through quartz or alumina tubes at the indicated temperatures	60
4.27	Input and output data for the program CMEM	64

List of Figures

Number		Page
1.1	Removal of contaminant gases from IGCC gases using a high temperature membrane.	2
1.2	Mechanism of facilitated transport of H ₂ S in a molten carbonate membrane	4
3.1	Schematic diagram of high temperature, high pressure absorption and membrane system	9
3.2	Schematic diagrams of membrane test cells.	15
4.1	Log K plots for reactions of pure carbonate salts	19
4.2	TGA traces of Na ₂ CO ₃ obtained upon heating under a N ₂ atmosphere.	21
4.3	TGA traces of La ₂ (CO ₃) ₃	22
4.4	TGA traces of Eu ₂ (CO ₃) ₃	23
4.5	DTA trace of Cs ₂ CO ₃ upon heated under a N ₂ atmosphere	25
4.6	DTA traces of base composition carbonate mixture 30-A	29
4.7	Weight loss of ceramic powders after 24 hour exposure to molten carbonates	38
4.8	Sessile drop test system	40
4.9	Effect of sulfide ion content of mixed alkali carbonates on the contact angle on AlN	42
4.10	Effect of long term exposure on the contact angle of mixed alkali carbonates on AlN	43
4.11	Long term salt retention of aluminum nitride and lithium aluminate porous samples	46

Executive Summary

The successful development of advanced power generation systems such as Integrated Gasification Combined Cycle (IGCC) requires that practical methods for removal of gaseous and other contaminants be developed. Among numerous alternatives, membranes supply a method for the removal of contaminant gases.

A preferred gaseous separation scheme would involve removal of contaminant gases such as H_2S , HCl , NH_3 and others from the hot, high pressure fuel gas. Thus, the useful fuel gases such as H_2 , CO , and CH_4 would be recovered hot and at high pressure. Neither conventional polymeric membranes or microporous ceramic membranes can be used to accomplish the desired separation. Polymeric membranes are unstable at the high temperatures of IGCC gas mixtures and, in addition, generally permeate permanent gases, particularly H_2 , more readily than most contaminant gases. Microporous ceramic membranes likewise permeate H_2 more readily than contaminant gases.

The objective of this program was to demonstrate the feasibility of developing high temperature, high pressure, facilitated transport ceramic membranes to control gaseous contaminants in Integrated Gasification Combined Cycle (IGCC) power generation systems. Meeting this objective requires that the contaminant gas H_2S be removed from an IGCC gas mixture without a substantial loss of the other gaseous components, specifically H_2 and CH_4 . As described above, this requires consideration of other, nonconventional types of membranes. The solution evaluated in this program involved the use of facilitated transport membranes consisting of molten mixtures of alkali and alkaline earth carbonate salts immobilized in a microporous ceramic support.

To accomplish this objective, Air Products and Chemicals, Inc., Golden Technologies Company Inc., and Research Triangle Institute worked together to develop and test high temperature facilitated membranes for the removal of H_2S from IGCC gas mixtures. Three basic experimental activities were pursued:

- (1) evaluation of the H_2S chemistry of a variety of alkali and alkaline earth carbonate salt mixtures
- (2) development of microporous ceramic materials which were chemically and physically compatible with molten carbonate salt mixtures under IGCC conditions and which could function as a host to support a molten carbonate mixture and
- (3) fabrication of molten carbonate/ceramic immobilized liquid membranes and evaluation of these membranes under conditions approximating those found in the intended application.

Results of these activities are summarized below.

A series of mixtures consisting of alkali and alkaline earth carbonate salts were prepared and characterized by a variety of techniques including thermal gravimetric analysis (TGA) and differential thermal analysis (DTA). Seven of these exhibited properties suitable for use in a high temperature immobilized liquid membranes, melting points below 600°C and nonvolatility under CO₂ at temperatures to 840°C. It was further shown that incorporation of sulfide ion in concentrations as high as 25 mole % resulted in molten mixtures at 600°C or lower. That sulfide-containing mixtures are liquid at reasonable temperatures is critical to the success of molten carbonate membranes for removal of H₂S. Partial solidification of the melt could result in membrane failure.

Since carbonate membranes permeate H₂S by a facilitated transport mechanism, a knowledge of the reactivity of H₂S with the carbonate mixtures was required for choice of the optimal membrane material. For this reason, an evaluation of the equilibrium constant for the reaction of H₂S with molten carbonate mixtures was carried out by a series of absorption experiments. This activity was complicated by several experimental difficulties. The most serious of these was the reactivity of H₂S with the metal test apparatus at the high temperatures used.

Such reactivity made collection of meaningful information quite difficult.

However, a reasonable equilibrium constant for the reaction of H₂S with one carbonate melt was determined, 0.235 atm at 560°C.

Through a process involving literature searches and screening experiments, it was determined that aluminum nitride and lithium aluminate were the best candidate ceramics for use as microporous supports for immobilized molten carbonate membranes.

Aluminum nitride discs and tubes with pore sizes in the range 0.38-0.42 μm with 45-50% open porosity were successfully produced. These discs and tubes were infiltrated with a molten carbonate mixture using techniques developed for this program. In the course of this work, it was determined that boron nitride can be used as a coating to help control the infiltration process of these materials. While lithium aluminate had better long term stability than aluminum nitride in contact with the molten carbonates, fabrication of discs of this material with pore sizes in the range required to contain the molten carbonate mixtures was unsuccessful. This was because of limited source suppliers of lithium aluminate powders and the inability to reduce the starting particle size of commercially available powders without introducing excessive mill/media contamination.

Three types of molten carbonate membranes were prepared. These consisted of a carbonate mixture immobilized in a microporous gold frit, in a planar microporous ceramic support, or in a tubular microporous ceramic support. A significant problem relating to membrane testing involved the tendency of planar ceramic membranes to crack upon sealing in the membrane cell. Membrane cracking was minimized by sealing using a graphite tape technique. Testing of molten carbonate membranes at 560°C and using H₂S containing feeds at relatively low flow rates was complicated greatly by the reactivity of H₂S with the membrane cell. As for the absorption experiments above, consumption of H₂S by reaction with metal led to unreliable determinations of H₂S permeabilities. This is a serious problem which would need to be addressed in future

work. Membrane cells could be constructed of quartz or alumina which were shown to be inert with respect to H_2S at temperature to $700^\circ C$.

Due to the problem of H_2S -metal reactivity, molten carbonate/planar ceramic membranes were evaluated using feeds which contained no H_2S . For most of the membranes so examined, gas permeance were quite high indicative of defects in the molten carbonate layer. This is, of course, a serious problem that would need to be addressed further. However, for a few membranes, reasonable, but still somewhat high, CO_2 permeabilities; for example 1,200 Barrers, were obtained suggesting that the fabrication of largely defect-free membranes is possible.

Some of the difficulties of H_2S -metal reactivity were minimized through testing at significantly higher gas flow rates. Permselective testing was performed using membranes consisting of a molten carbonate mixture in planar and tubular ceramic supports. Erratic membrane performance was observed. Often, H_2 or helium permeabilities were much higher than those predicted based on a solution-diffusion mechanism indicative of defects in the molten carbonate layer. However, in some instances H_2S to H_2 or He selectivities greater than one were observed. Based on fairly limited data, an observed decrease in H_2S permeability with increasing feed pressure was consistent with facilitated transport of H_2S . Examination of membranes after testing revealed that there apparently is a tendency for the melt to migrate in or out of the support. This was particularly apparent for tubular membranes where the salt appeared to have migrated downward along the tube. Planar ceramic membranes examined after testing showed evidence of regions of unfilled pores near the middle of the discs. In addition, for one unused planar ceramic membrane, similar unfilled regions were observed as well.

1.0 Background

The successful development of advanced power generation systems such as Integrated Gasification Combined Cycle (IGCC) requires that practical methods for removal of gaseous and other contaminants be developed. Among numerous alternatives, membranes supply a method for the removal of contaminant gases. As illustrated in Figure 1.1, the preferred gaseous separation scheme would involve removal of contaminant gases such as H_2S , HCl , NH_3 and others from the hot, high pressure fuel gas.¹ Thus, the useful fuel gases such as H_2 , CO , and CH_4 , would be recovered hot and at high pressure.

Application of conventional gas separating membranes to such a separation scheme is impractical. Generally, such membranes consist of organic polymers which cannot be used at the high temperatures of IGCC gas mixtures. Further, conventional polymeric membranes generally permeate permanent gases, particularly H_2 , more readily than most contaminant gases.² Thus, the permselective properties of conventional polymeric membranes are unsuitable for removal of a contaminant such as H_2S from a gas mixture rich in H_2 .

Microporous ceramic membranes, unlike polymeric membranes, are stable at the high IGCC temperatures. However, the permselective properties of these membranes are also not suited to the separation scheme illustrated in Figure 1.1. Microporous ceramic membranes permeate gases such as H_2 more readily than contaminants such as H_2S and the desired separation is not obtained.³

The specific problem addressed in this program was the development of membranes which selectively permeate H_2S from hot fuel gas while leaving the other gases in the stream largely unaffected. Development of such a membrane requires consideration of other, nonconventional types of membranes. The solution evaluated in this program involved the use of facilitated transport membranes. Facilitated transport membranes are systems in which permeation of a specific gas is augmented by means of a reversible chemical reaction or interaction with the membrane material. Other gases do not react with the membrane and, hence, are far less permeable. Generally speaking, facilitated transport membranes have historically consisted of a reactive liquid immobilized in a porous support.⁴ For example, Air Products has developed a family of facilitated transport membranes which selectively permeate acid gases at ambient temperatures.⁵ These membranes consisted of an acid gas reactive liquid immobilized in the pores of a microporous polymeric support. The reversible reactivity of the liquid with CO_2 or H_2S resulted in high permeabilities of these gases. Gases such as H_2 or CH_4 have low solubilities in the membrane liquid and, since they permeate by a solution-diffusion pathway, their permeabilities are quite low. Thus, an effective separation of acid gases from H_2 or CH_4 can be obtained. Such membranes, although useful at room temperature, are of no value at the high temperatures and pressures found in fuel gas separations. Nonetheless, the concept can be applied successfully if the "right" reactive liquid and support can be found.

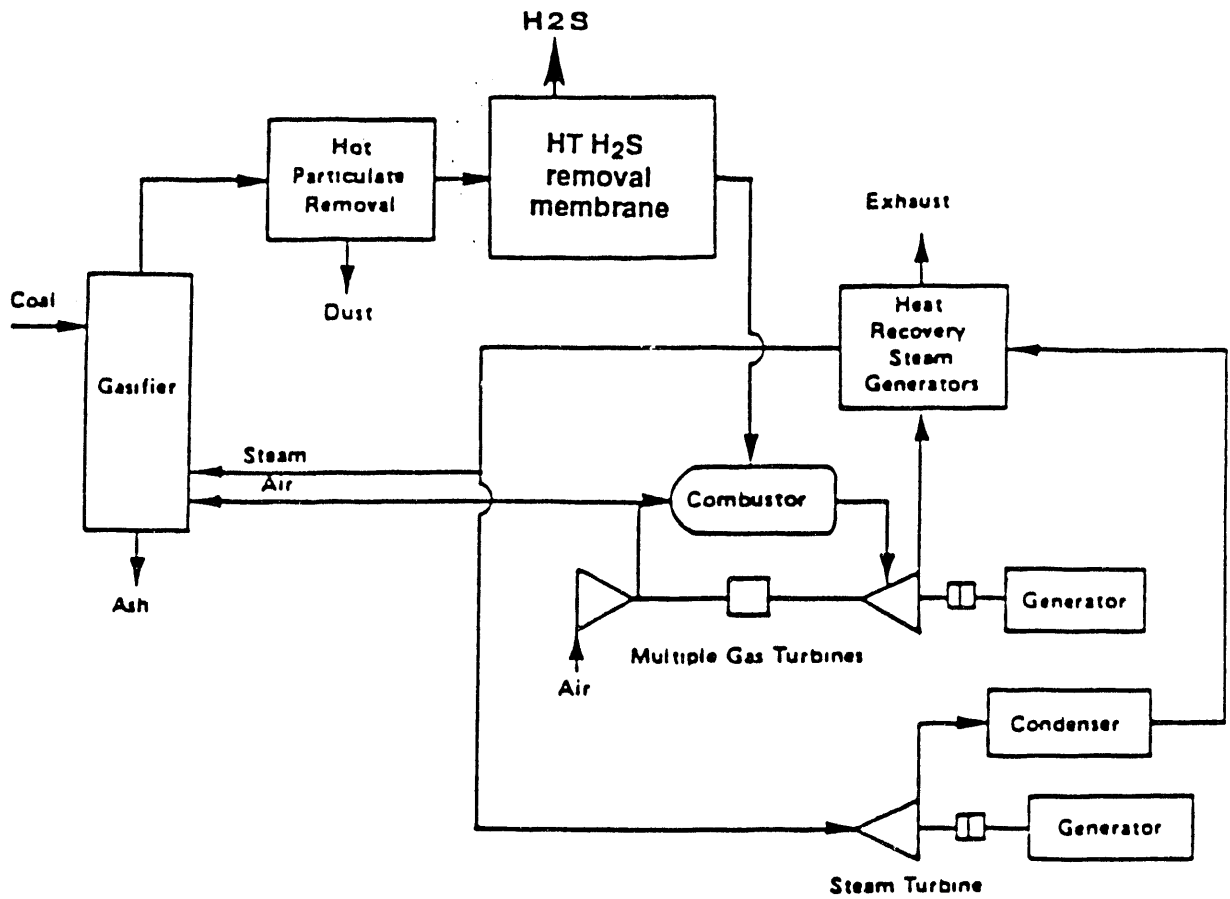
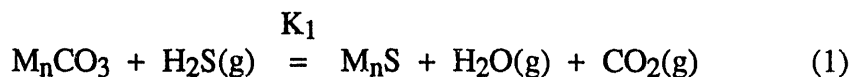


Figure 1.1 Removal of contaminant gases from IGCC gases using a high temperature membrane.

The requirements for the right materials are fairly stringent. The reactive liquid must be stable and involatile at high temperature, 500-800°C. In addition, the liquid must react reversibly with H₂S at the pressures found in fuel gases. The support must be inert with respect to the reactive liquid and the fuel gas at elevated temperature and be relatively thin. It must have sufficiently small pores to maintain thin liquid films at high pressures. After examination of the available literature, carbonate salt mixtures were chosen as the reactive liquid and microporous ceramics were chosen as the support.

It is known that carbonate salts react reversibly with H₂S as represented by reaction (1) where M represents a monovalent metal cation and n is 1 or 2:⁶



In addition, although most pure carbonate salts are not molten at a temperature reasonable (e.g. K₂CO₃, mp. 898°C⁷) for use in an immobilized liquid membrane, many examples of relatively low melting mixtures of alkali and alkaline earth carbonates are known. For example, a mixture containing 44.1 mole% Li₂CO₃, 29.8 mole% Na₂CO₃, and 26.1 mole% K₂CO₃ melts at 393°C.⁷ Mixtures of carbonate salts possess the reversible H₂S reactivity and melting points required for a successful facilitated transport membrane.

Various carbonates and carbonate mixtures have been extensively evaluated as absorbents for H₂S. Moore,⁸ Stegen,⁹ and Lyke¹⁰ and their coworkers have shown carbonate melts to be effective absorbents of H₂S from hot fuel gas mixtures and at least two US patents claiming the use of carbonate melts as H₂S absorbents have appeared.^{11,12} Absorption occurs by the chemistry of reaction (1). Equilibrium constants and enthalpies of reaction for reaction (1) involving carbonate melts containing lithium, sodium, potassium, and calcium cations were determined and at 750°C ranged from 1.6 to 2.0 atm. Regeneration of the H₂S free absorbent is accomplished by exposure to CO₂ and steam which results in reaction (1) proceeding in the reverse direction.

The mechanism of permeation of H₂S in a molten carbonate membrane is shown schematically in Figure 1.2. At the feed interface, where the pressure of H₂S is relatively high, H₂S reacts with carbonate ions as in reaction (1) to form sulfide ions in the melt and H₂O and CO₂ which are liberated into the gas phase. The sulfide ions diffuse in a concentration gradient to the low pressure side (permeate) of the membrane. Here, a sweep gas containing CO₂ and H₂O causes reaction (1) to occur in the reverse direction. H₂S is formed, released into the gas phase and removed from the permeate interface by the sweep gas. This is accompanied by "regeneration" of the melt to the carbonate form. The other gases in the feed fuel gas, H₂, CO, CH₄ and others, do not react chemically with the melt. Permeation of these gases can only occur by a solution-diffusion mechanism in which gases physically dissolve as discrete molecules and diffuse from the high to the low pressure side of the membrane. Since the solubility of gases such as H₂ are expected to be low in the highly ionic carbonate melts, permeabilities of these gases

are likewise expected to be low. Thus, in principle, a selective removal of H_2S without substantial loss of other fuel gases can be achieved.

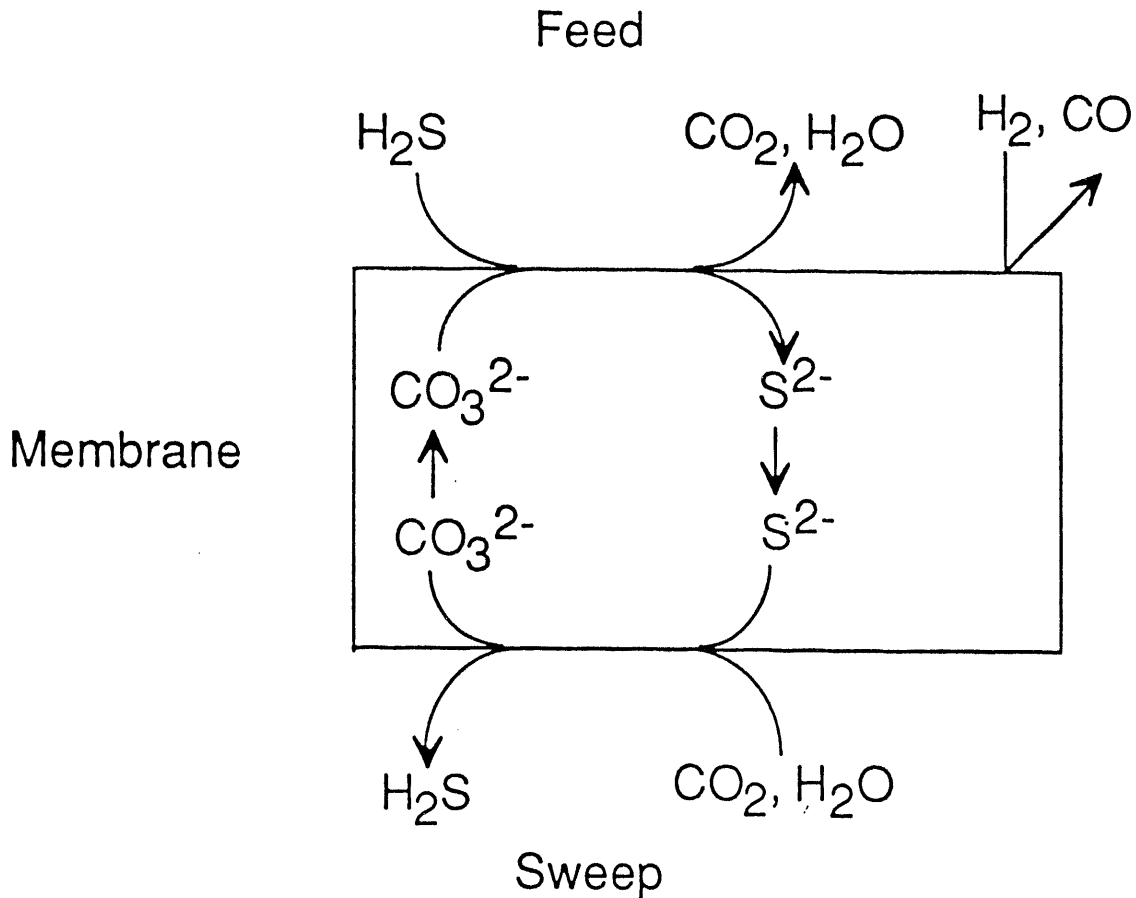


Figure 1.2 Mechanism of facilitated transport of H_2S in a molten carbonate membrane. Membrane is viewed in cross-section.

The high operating temperatures (500-800°C) combined with the range of oxidative conditions (very low on feed side and moderate on the sweep side of the membrane) present a significant challenge for selection of the microporous support material. The highly corrosive nature of the molten alkali carbonates makes that selection even more difficult. Metals and metallic alloys, especially in the very high surface area form required in a microporous support, will not be suitable due to their tendency toward oxidation and corrosion. Ceramic materials, on the other hand, possess the desirable combination of high temperature strength, corrosion resistance, and the ability to form high void fraction microporous supports. Crystalline ceramics are known to maintain their strength and elastic stiffness to near their melting temperature, which for most ceramics of interest to this program is greater than 1200°C. The corrosion resistance of ceramics is also well documented, with ceramics used in the processing of molten metals and glasses and in such severe environments as molten cryolite. In addition, substantial progress has been made in recent years to develop microporous ceramics for use as membranes for the separation of liquids and gases.

2. Objectives and Project Description

2.1 Objectives

The objective of this project was to demonstrate the feasibility of developing high temperature, high pressure, facilitated transport ceramic membranes to control gaseous contaminants in Integrated Gasification Combined Cycle (IGCC) power generation systems. Meeting this objective requires that the contaminant gas hydrogen sulfide, H₂S, be removed from an IGCC gas mixture without substantial loss of the other gaseous components, specifically hydrogen, carbon monoxide, and methane.

2.2 Program Description

To accomplish the above objectives, Air Products and Chemicals, Inc., Golden Technologies and Research Triangle Institute worked together to develop and test high temperature facilitated membranes for the removal of H₂S from IGCC gas mixtures. The work involved in this program can be grouped into four tasks: (1) test plan preparation (2) concept evaluation, development and testing (3) feasibility demonstration and (4) process performance, evaluation and economics. The test plan formulated was reported previously. Due to some very serious experimental problems, limited work relating to Tasks 3 and 4 was completed and the current report describes largely the results of Task 2 activities.

Task 2 consisted of three basic activities. The first of these involved the determination of equilibrium constants for the reaction of H₂S with various molten alkali and alkaline earth carbonate salt mixtures. In addition, immobilized molten carbonate membranes were to be prepared and evaluated for the removal of H₂S from gas mixtures. Further, a model to predict the permselective properties of molten carbonate membranes was to be developed with the intent of determining the required H₂S-molten carbonate reactivity for optimal permselective properties.

A second activity pursued in parallel involved the development of ceramic materials which were chemically and physically compatible with molten carbonate salt mixtures under IGCC conditions. A microporous ceramic host capable of supporting a molten carbonate mixture was to be developed and appropriate immobilized liquid membranes were to be fabricated.

Thirdly, the permselective properties of these molten carbonate/ceramic immobilized liquid membranes were to be evaluated under conditions approximating those found in the intended application. The results of this evaluation would then provide a basis for assessing the technical feasibility of the concept.

3.0 Experimental Section

3.1 Salt mixture preparation and characterization

3.1.1 Methods

Differential thermal analysis (DTA) data was obtained using a DuPont 1600 differential thermal analysis analyzer. The sample was contained in a platinum cup. The reference cup was filled with alumina. The sample chamber was purged with CO₂ or N₂ as indicated as a flow rate of 100 cc/min. Data was collected from ambient to 1000°C at a heating rate of 20°C/min.

Thermal gravimetric analysis (TGA) data was obtained using a Perkin-Elmer 7 Series Thermal Analysis System. Samples were contained in a platinum pan and the sample compartment was purged with CO₂ or N₂ as indicated at a flow rate of 50 cc/min. Generally, data was collected from between 30 and 830°C at a heating rate of 40°C/min. Exceptions are noted in the text.

3.1.2 Materials

Prior to use, as received carbonate salts were heated under flowing CO₂ for 18 hours at 300°C in dense alumina crucibles. Following heating, the aluminum ion content of each salt was quite low, <0.04%, confirming that no contamination from the crucible had occurred.

Mixture preparation. Each mixture was prepared using the following general procedure. Weighed quantities of the appropriate salts were ground into a mixture of a fine powders using a mortar and pestle. The mixture was transferred into a gold crucible and was heated under an atmosphere of CO₂ at 300°C for 4 hours and 550°C for 4 hours. The molten mixture was poured from the hot crucible into an aluminum pan at room temperature, causing immediate solidification. The solid was ground into a fine powder and heated to 300°C under CO₂ to remove absorbed water. It was subsequently stored under a dry, inert atmosphere. Exceptions to this general procedure and other information specific to the preparation of individual mixtures are noted below. Mixture compositions are listed in Table 3.1.1 below.

Table 3.1.1. Compositions and melting temperatures of carbonate mixtures prepared.

	<u>Composition, mole %</u>									
	30-A	34-1	27-1	23-2	31-1	32-1	34-2	25-2	26-1	40-1
<u>Components</u>										
Li ₂ CO ₃	49.0	37.36	35.29	32.98	32.87	33.27	35.34	34.67	36.42	
K ₂ CO ₃	25.2	19.26	21.82	22.38	22.22	22.40	21.74	22.19	22.59	33.23
CaCO ₃	25.7	20.06	23.71	25.06	25.01	24.73	23.69	23.42	22.81	
Na ₂ CO ₃		23.30								33.09
Rb ₂ CO ₃			19.59							

Cs ₂ CO ₃				19.19						33.68
SrCO ₃					19.89					
BaCO ₃						19.60				
MnCO ₃							19.23			
La ₂ (CO ₃) ₃								19.72		
Eu ₂ (CO ₃) ₃									18.18	
MP(°C)	485	405, 449	447, 482	426, 443	481	469	*	*	*	429, 546

* Unstable at or below melting point

Prior to heating at elevated temperatures, mixture 23-2 was heated overnight under CO₂ at 130°C.

When mixture 32-1 was heated to 550°C, some solid remained. Additional heating at 650°C for 4 hours resulted in a fully molten sample.

Mixtures 25-2 and 26-1 were heated under flowing CO₂ at 300°C for 4h and 550°C for 2h. Neither sample appeared to be molten at 550°C. Heating to 600°C for 1.5h did not result in melting for either mixture. After cooling under CO₂, it was determined that mixture 25-2 had lost 7.1% of its initial weight and mixture 26-1 had lost 54.1%.

For mixture 40-1, additional heating at 600°C for 2h was required to obtain a fully molten sample. To transfer the liquid from the crucible, the temperature was raised to 650°C briefly.

Mixture 34-2, which contained MnCO₃, was heated to 300°C for 4h and then to 550°C. The mixture formed a deep brown/red liquid which appeared to be evolve gas. Heating was ended.

Preparation of mixtures containing sulfide ions. Sulfide-containing mixtures were prepared by a procedure similar to that described above. Weighed quantities of Li₂CO₃, K₂CO₃, CaCO₃, and CaS (Matthey Electronics, 99.99%) were ground into a fine powder using a mortar and pestle. The amount of CaCO₃ was adjusted to keep the Li/K/Ca molar ratio the same as that of the base composition. For mixtures containing about 25% CaS, no CaCO₃ was used. Mixtures were transferred into gold crucibles and heated under flowing CO₂ at 300°C for 1h, 550°C for 1/2h and 600°C for 3h. All the samples appeared to be liquid at this temperature but each were somewhat colored with a small amount of a gold colored solid, most likely iron sulfide, floating on the surface. The molten mixtures were poured into aluminum pans at room temperature, which resulted in immediate solidification. The samples were ground into a powder under an inert atmosphere.

Mixtures 46-1 and 46-2 were prepared by heating to 100°C overnight, 550°C for 2 h, and 600°C for 2 h under flowing CO₂ rather than at the above cited temperatures.

3.2 Absorption Experiments.

The apparatus used to perform absorption experiments is shown schematically in Figure 3.2. A detailed drawing of this apparatus and listing of the components can be found in the Appendix. Details of each individual absorption experiment are listed below.

Feed mixtures were prepared by transferring known pressures of gas into an initially evacuated mixing vessel. H₂S was transferred into the vessel first, followed by CO₂ and then other permanent gases. Prior to initiating experimental work, it had been intended to introduce water vapor by adding liquid water to the evacuated mixing vessel and heating to vaporization. However, experiments using water containing gas mixtures were not performed. When the addition of gases was complete, the mixing vessels were heated to 70°C and the contents were stirred with a paddle stirrer. All gas lines leading from the mixing vessels were heat traced and maintained at 70°C. The dosing and sampling containers were stainless steel vessels which were also heat traced. The volumes of the dosing volume and sample volume were determined by expansion of gas from a calibrated volume and were 0.5124L and 0.1857 L, respectively. Molar quantities of gases transferred or absorbed were calculated based on the assumption that all gases are ideal.

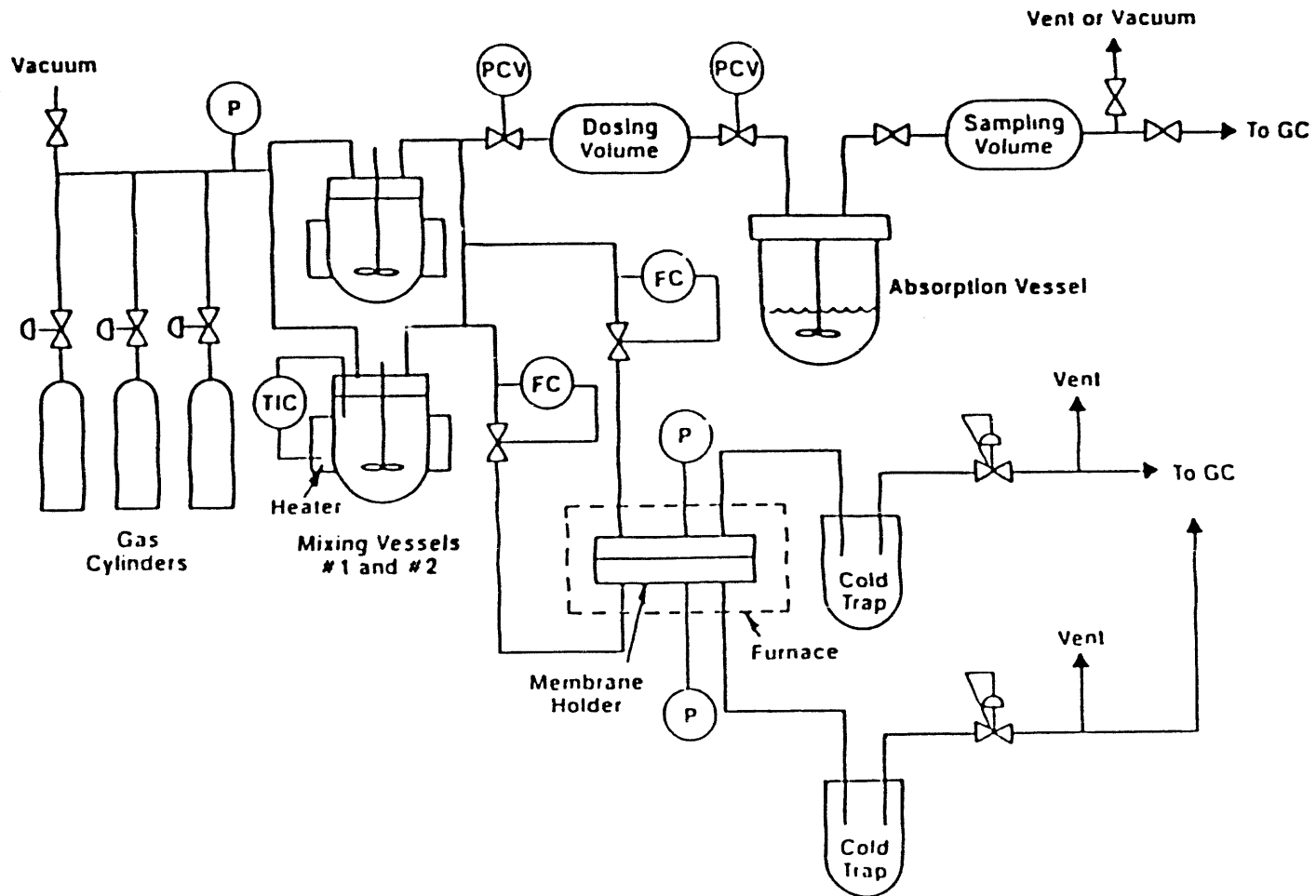


Figure 3.1 Schematic diagram of high temperature, high pressure absorption and membrane system.

The absorption vessel consisted of a one liter Parr reactor designed for operation at pressures and temperatures to 1000 psi and 800°C. The reactor body, head, and thermowells were constructed of Incoloy 800 HT. The contents of the reactor were heated by cartridge heaters inserted into the exterior of the thermowells. The internal surface of the reactor was lined with a ceramic tube with a wall thickness of about 0.2 in. The bottom of the reactor was lined with a ceramic disc of about the same thickness. Inside the ceramic lining was placed a cylindrical gold vessel. The purpose of the gold vessel was to provide an inert container for the carbonate melts upon exposure to H₂S.

To analyze the gas phase of the absorption vessel, an aliquot of gas was withdrawn into the sampling volume. Following pressurization with N₂, the sample was analyzed in a Hewlett Packard GC operating at an oven temperature of 80°C. Columns and configurations as listed in Appendix. This configuration of the GC permitted detection and quantification of H₂, CO, CO₂, H₂S, COS, and CH₄.

Absorption experiment 12666-2. The intent of the experiment was to expose the base composition carbonate mixture to a gas mixture containing only H₂S and CH₄. However, due to a mechanical problem or back contamination of gases of unknown origin, the feed mixture used contained H₂ as well. The composition of the feed mixture as determined by GC was 10.7% H₂S, 6.40% CO₂, 81.1% CH₄, and 1.8% H₂. The absorption vessel was loaded with 124.81 g (1.2899 mole CO₃²⁻) of the base carbonate mixture 30-A. The absorption vessel was heated to 560°C and stirring of the melt was begun. The dosing and sample volumes were maintained at 75°C.

The volume of the absorption vessel available to gas was determined by helium expansion from the dosing volume and was 0.7636 L. The volumes of the dosing volume and sample volume, as determined previously using a calibrated gas volume, were 0.5124 and 0.1857 L, respectively. The feed gas mixture was added to the evacuated dosing volume to a pressure of 402.3 psia. A portion of this gas was added to the absorption vessel such that the final pressure of the dosing volume was 287.5 psia. This pressure change corresponds to 0.1401 moles of gas transferred into the absorption vessel. After 12 hrs, the pressure in the reactor dropped from 248.8 psia initially to 240.6 psia at equilibrium. A portion of the headspace gases was withdrawn into the evacuated sample volume to a pressure of 51.8 psia (0.0229 moles). This mixture was pressurized with N₂ to a total pressure of 616.0 psia and analyzed by GC revealing the following gas concentrations in ppm:

	<u>ppm</u>	<u>mole fraction</u> <u>(see below)</u>
H ₂ S	80.8	9.608x10 ⁻⁴
CO ₂	2,678	3.185x10 ⁻²
CH ₄	64,665	7.692x10 ⁻¹
CO	7,567	8.998x10 ⁻²
COS	8.3	9.809x10 ⁻⁵
H ₂	5,941	7.065x10 ⁻²
H ₂ O	-	3.726x10 ⁻²

Using the above values of gas concentration, the quantity in moles of each component withdrawn into the sample volume were calculated and summed. Assuming that water is only gas which was present and not quantified by GC, the concentration of water is given by the difference between the above sum and the quantity of gas as determined by the ideal gas law. Mole fractions corresponding to the gas composition at equilibrium were calculated and are displayed above.

The quantity of H₂S absorbed at equilibrium corresponds to the quantity of H₂S added to the absorption vessel minus that remaining at equilibrium or 1.48x10⁻² moles.¹² Hence, at equilibrium the salt mixture contains 1.48x10⁻² moles of S²⁻. The quantity of CO₃²⁻ is given the initial quantity of CO₃²⁻ minus the quantity of sulfide at equilibrium or 1.249 mole CO₃²⁻. Substituting the appropriate values in equation (12) yields K = 3.448 psia or 0.235 atm:

$$K = P \cdot \frac{x_{H_2O} \cdot x_{CO_2}}{x_{H_2S}} \cdot \frac{n(S^{2-})}{n(CO_3^{2-})}$$

Absorption experiment 12666-6. A gas mixture of the composition 8.382% H₂S, 40.36% CO₂, 51.28% CH₄, as determined by GC, was used to perform a second absorption experiment. To the absorption vessel was added 134.2 g of the base carbonate mixture (1.3869 mole CO₃²⁻), which was heated to 560°C. The dosing volume was pressurized to 420.3 psia with the feed gas mixture. A portion of this was transferred into the absorption vessel such that the final pressure of the dosing volume was 275.7 psia or 0.17642 moles of gas were transferred. After standing overnight, the pressure in the absorption vessel was 225.0 psia. A portion of the gas phase was transferred to the sample volume (74.1 psia) and pressurized with N₂ to a total pressure of 798.6 psia. Analysis by GC gave the following composition:

Gas	conc. (ppm)
H ₂ S	475.1
CO ₂	30163
CH ₄	51120
CO	25789
COS	64.8
H ₂	4072
H ₂ O	-

When the quantities of gases in the above table were used to calculate quantities in moles and were summed, the value obtained was greater than the number of moles of gas withdrawn into the sample volume. Hence, a quantity of H₂O, and thus an equilibrium constant, could not be calculated. Presumably, this arises from the relatively larger error in the sum of the individual gases.

Absorption experiment 12666-15. The absorption properties of the base carbonate mixture were determined using a feed gas containing only H₂S and CO₂. Although an inadvertent valve switch precluded a quantitative treatment, the data were provided a basis for comparison. A 126.9 g sample of the base composition carbonate mixture was heated to 560°C in the absorption vessel. The melt was then exposed to a gas mixture containing 15.0% H₂S in CO₂. After standing overnight, a portion of the headspace gases was withdrawn into the sample volume to a pressure of 102.9 psia, pressurized with N₂ to a total pressure of 803.1 psia, and analyzed by GC. The following gases were detected in the indicated quantities:

Gas	conc (ppm)
H ₂ S	2,710
CO ₂	116,600
CO	25,060
COS	130
H ₂	2,690

Absorption experiment 12923-32. One additional absorption experiment was performed following gold plating of the various components of the absorption vessel. Feed gas containing 0.5% H₂S in N₂ was added to 125.8 g of the base carbonate mixture 30-A at 550°C. This was dosed into the reactor, and the system was allowed to come to equilibrium. Some gas was removed into the sampling volume (69.8 psia) and pressurized to 805.9 psia with N₂. Analysis of this gas revealed the following gas concentrations: CO₂, 2419 ppm; CO, 1306 ppm; CH₄, 1063 ppm; H₂, 1121 ppm. H₂S and COS were not detected. Assuming that no water is present in the gas phase, the concentration of gases at equilibrium were: CO₂, 2.82%; CO, 1.52%; CH₄, 1.24%; H₂, 1.30%.

Gas phase reactivity in the absence of a molten carbonate mixture. The absorption vessel with the gold liner was partially filled with sand as a thermal sink and heated to 550°C. The absorption vessel was pressurized to 111.9 psia with a mixture containing 32.1% CO₂, 46.5% H₂, and 21.4% CH₄. After standing overnight, the pressure dropped slightly to 107.0 psia. A portion of the gas phase was removed, pressurized with N₂, analyzed by GC and found to contain CO in addition to the three original gases. Assuming that no other gases were present with the exception of the diluent N₂, the following concentrations of gases were present in the absorption vessel: 20.9% CO; 16.5% CO₂; 40.0% H₂; 22.6% CH₄. It is likely that H₂O was also present but it was not quantified. Following cooling to room temperature, visual examination of the absorption vessel revealed no black deposits.

Estimation of errors in the determination of quantities of gas. To establish the accuracy with which quantities of gas absorbed could be determined, a blank experiment involving helium gas at 27°C was performed. Following determination of the absorption vessel volume by expansion of gas from the dosing volume, the absorption vessel was pressurized with helium to 100.1 psia which corresponded to 0.258 mole of gas.

Transfer of a portion of this gas into the evacuated sample volume resulted in an absorption vessel pressure of 92.1 psia or 0.237 moles remained. The pressure of the sample vessel was 34.3 psia which corresponded to 0.0176 moles. Based on this value, the quantity of gas remaining in the absorption vessel should be 0.240 moles or a 0.0034 mole discrepancy or about a 1.5% error. Realistically, this is a minimum error and larger errors can be expected at the actual operating temperature of the unit.

3.3. Membrane preparation and testing

3.3.1 Membrane testing. The apparatus used to evaluate the permselective properties of molten carbonate membranes is shown schematically in Figure 3.1. A detailed drawing of this apparatus and a listing of the components is in the Appendix. Two gas mixtures, a feed and a sweep gas, were prepared in the mixing vessel as described above. Initially, it had been intended to add liquid water to the mixing vessels and heat to vaporization, but it was subsequently decided to humidify the feed and sweep gases by passage through bubblers containing water, usually at 60°C. These bubblers are not shown in Figure 3.1. After the mixing, all gas line vessels were heat traced and maintained at 80°C. Feed and sweep gas flows were set using mass flow controllers. However, it was found that exposure of these controllers to corrosive gases at 80°C resulted in numerous instances of controller failure, and they were replaced with needle valves. The membrane to be tested was held in a membrane cell constructed of stainless steel and illustrated in Figure 3.2. Different cells were used for molten carbonate/gold frit and planar molten carbonate/ceramic membranes and both are shown in Figure 3.2. Some membranes were examined using the same holder following gold plating of surfaces exposed to gas. The membrane cell was heated to the operating temperature, usually 560°C, in a furnace. Downstream from the membrane unit were back pressure regulators which could be set to obtain either feed or sweep pressures greater than ambient. Pressures of both gases were determined by the use of pressure transducers. Either the feed or sweep gas could be directed to the GC for analysis as described in Section 3.2.

Ceramic based membranes were sealed in the membrane cell using either a gold plated O-ring or C-ring. Sealing was accomplished by contact of the O- or C-ring with the surface of the membranes. The use of a C-ring resulted in a greater frequency of crack-free membranes. For later membranes, an alternative approach utilized graphite tape. In an initial attempt, 3/8" wide, 0.005" thick graphite tape was applied to the edges and part of the faces of an AlN/salt membrane. An inner C-ring was not used. Examination of the membrane after testing suggested that removal of the inner C-ring groove would supply more appropriate surfaces for sealing to graphite tape. This was done and subsequent membranes were sealed by the use of circular graphite gaskets which were laid on the faces of the membrane.

Permeabilities of molten carbonate/gold frit membranes were calculated assuming that the membrane area and thickness are those of the gold frit, 1.13 cm² and 0.1639 cm. No correction for porosity or tortuosity was applied.

Permeabilities of carbonate/ceramic membranes were calculated assuming that the membrane area and thickness were those of the ceramic support: 4.31 cm² and 0.254 cm. A porosity of 50% was assumed. No correction for tortuosity was applied.

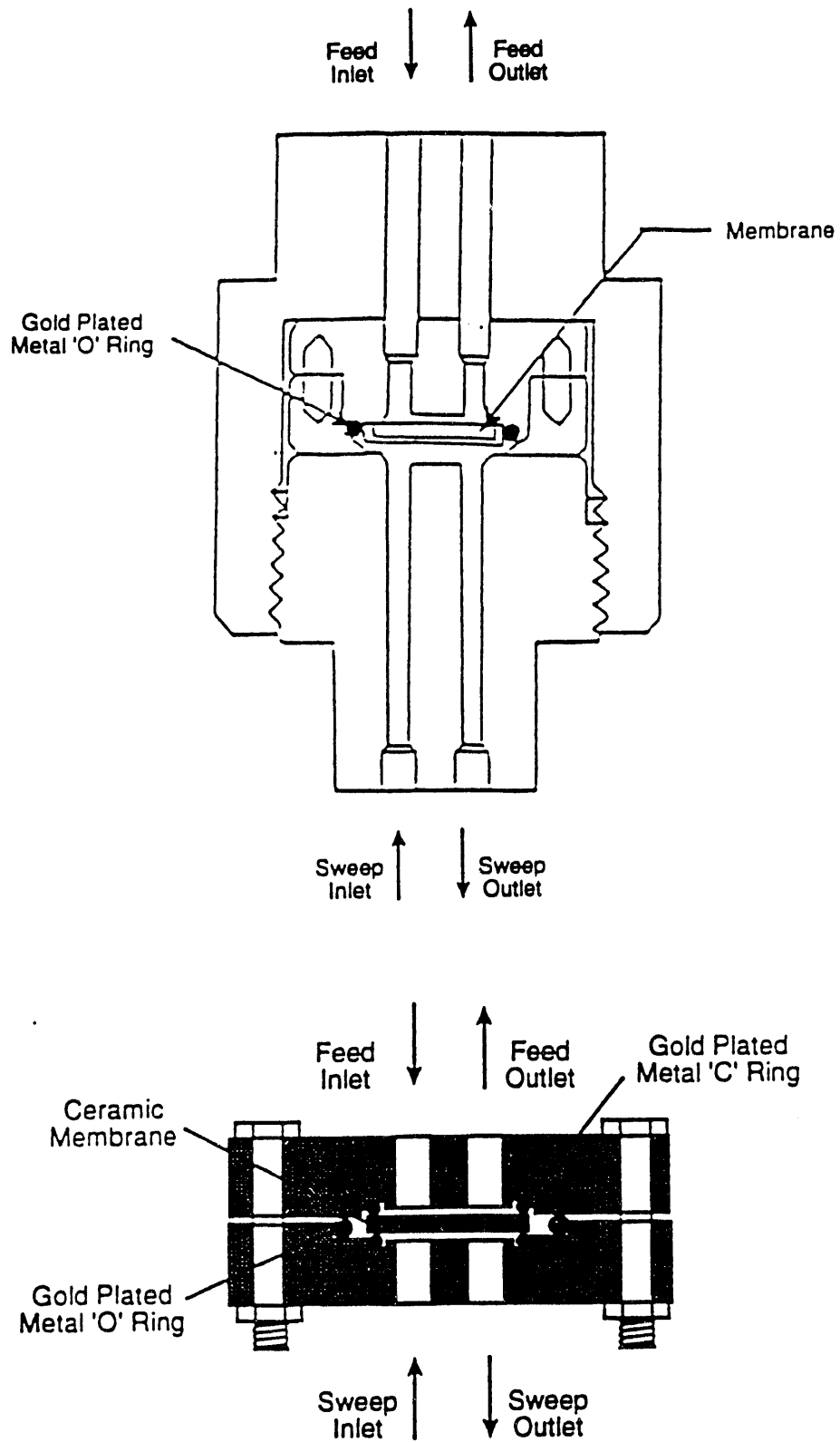


Figure 3.2 Schematic diagrams of membrane test cells.
 Top: Cell used for molten carbonate/gold frit membranes.
 Bottom: Cell used for planar molten carbonate/ceramic membranes.

3.3.2 Membrane preparation

Preparation of molten salt membranes supported in gold frits. A weighed quantity of the base carbonate mixture 30-A was placed on the surface of a gold frit containing $0.5\mu\text{m}$ pores and was heated to 550°C under flowing CO_2 . After cooling to room temperature, no salt was observed on the bottom surface of the frit. A small residue of salt was observed on the top surface, and it was removed by scrapping it off. Several membranes were prepared in this manner. Two were used for testing: membrane 11818-47-2 containing 0.0755g of the base composition and membrane 11818-54-2 containing 0.0655 g.

Preparation of molten salt membranes supported in microporous ceramic planar discs. The infiltration process for planar discs involved placing the porous ceramic disc into a boat fashioned out of gold foil. Powdered salt was then added. The amount of salt added was calculated to be 25% in excess of that needed to completely fill the open pore volume of the ceramic disc. The foil boat containing the disc and salt were then placed in a retort furnace. The furnace was evacuated and backfilled to 1atm with CO_2 twice. The furnace was heated to $\sim 700^{\circ}\text{C}$ under flowing CO_2 at which point the furnace was again evacuated and backfilled with CO_2 twice. The furnace was then cooled to room temperature under flowing CO_2 . In some cases, the ceramic disc was coated with a colloidal boron nitride (BN) spray prior to infiltration in an attempt to better control the infiltration (as discussed in Section 4.2.4). The principle underlying this method is that gases in the open pores are removed by evacuating the furnace. When the furnace chamber is then repressurized, the atmospheric pressure forces the molten salt into the pore volume of the ceramic. In addition, capillary forces ensure that the salt fills the smallest pores in the microstructure.

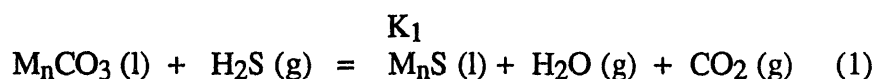
Preparation of molten salt membranes supported in microporous ceramic tubular supports. The infiltration of tubular membrane supports was performed in a way similar to that for discs; however, care had to be taken to prevent complete filling of the bore of the tube with the molten salts as this could lead to problems in removing the salts. This fixturing problem was resolved by placing a graphite rod slightly smaller than the tube ID down the bore of the tube. The end of the rod was wrapped with graphite tape to form a snug fit into the ends of the tube. This tube assembly was then placed into a boat fashioned from gold foil. The powdered salt was then added. In the case of the tubes, the amount of salt added was calculated to be 50% in excess of that needed to fill the open porosity, due to the larger surface area of the tubes. The actual infiltration was then accomplished in the same way as described above for the planar discs.

4.0 Results and Discussion

4.1 Development of molten carbonate salts.

The objective in the area of development of molten carbonate salts was to identify mixtures of carbonate salts which react reversibly with H₂S, CO₂ and H₂O under IGCC conditions. Such salts would then be used to fabricate immobilized liquid membranes which would selectively permeate H₂S from hot fuel gas streams. As described in Section 1.0, mixtures of carbonate salts were considered since the melting points of pure alkali or alkaline earth metal carbonates are generally higher than the expected temperature of membrane use, 500 to 850°C.

Efforts associated with development of molten carbonate mixtures involved an examination of available literature involving: (1) the reactivity of pure carbonates with H₂S, (2) the synthesis of new carbonate mixtures, and (3) the characterization of the physical and chemical properties of these mixtures. Chemical characterization involved a determination of the equilibrium constant for reaction (1) which occurs upon exposure of molten carbonates to H₂S. The value of K₁ can be determined by an absorption experiment which is discussed below.



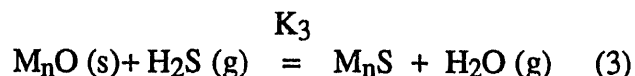
M = alkali or alkaline earth metal cation

n = 1 or 2

K₁ is the equilibrium constant of the reaction (1)

4.1.1 Survey of the H₂S reactivity of pure carbonate salts.

Before setting out on the synthesis of new carbonate melts, the thermodynamics of the reaction of pure carbonate salts with H₂S as in reaction (1) were examined. Reaction (1) can be thought of as occurring in two steps. The first, reaction (2), involved decomposition of the carbonate to yield the oxide and CO₂ gas. The oxide thus generated reacts with H₂S in an acid-base reaction, reaction (3).



The extent of reaction (1) depends on the equilibrium constants K₂ and K₃ since K₁ = K₂K₃. Hence, the less stable the carbonate (large K₂) and the more basic the oxide (large K₃), the greater will be the value of K₁. The available thermodynamic data (527-827°C) for alkali (Li, Na, K, Rb) and alkaline earth (Ca, Sr, Ba) salts were used to obtain log K

values which are plotted as a function of temperature in Figure 4.1.¹³ Values of K_2 and K_1 increase with increasing temperature while K_3 decreases. For illustrative purposes, $\log K$ at 627°C are listed below in Table 4.1.

Table 4.1. Log K values for reactions 1-3 at 627°C for pure alkali and alkaline earth carbonates.

metal cation	$\log K_2$	$\log K_3$	$\log K_1$
Li	-4.84	4.47	-0.37
Na	-10.99	9.79	-1.20
K	-14.86	15.58	0.72
Rb	-15.70	-	-
Ca	-1.96	3.64	1.68
Sr	-4.78	4.64	-0.14
Ba	-6.84	6.92	0.076

The above data suggests that Group I (alkali) carbonates are more stable than the corresponding Group II (alkaline earth) salts and stability increases down a group. Similarly, the basicity of oxides increases down a group and Group I oxides are more basic than Group II. The values of K_1 are less periodic in nature. Nonetheless, in the absence of literature data, it would appear that evaluation of Rb_2CO_3 or Cs_2CO_3 in carbonate mixtures would be worthwhile if larger K_1 values are required, especially at higher temperatures. It is reasonable to predict that Rb_2O and Cs_2O are among the most basic oxides and the presence of either carbonate in melts is expected to lead to large K_1 values.

4.1.2 Characterization of pure carbonate salts.

Prior to use in mixture preparation, the pure carbonate salts used were characterized by a variety of techniques. As received carbonate salts were heated under flowing CO_2 for 18 hr prior to use. To confirm the expected composition, the metal ion content of many of the salts was determined using atomic absorption analysis. These results are listed in Table 4.2 along with those for the as received salts. In general, agreement between theoretical metal ion content and that determined after heating were good. Satisfactory elemental analysis could not be obtained for $MgCO_3$. This coupled with its unusual thermal gravimetric properties led to discontinuation of its use.

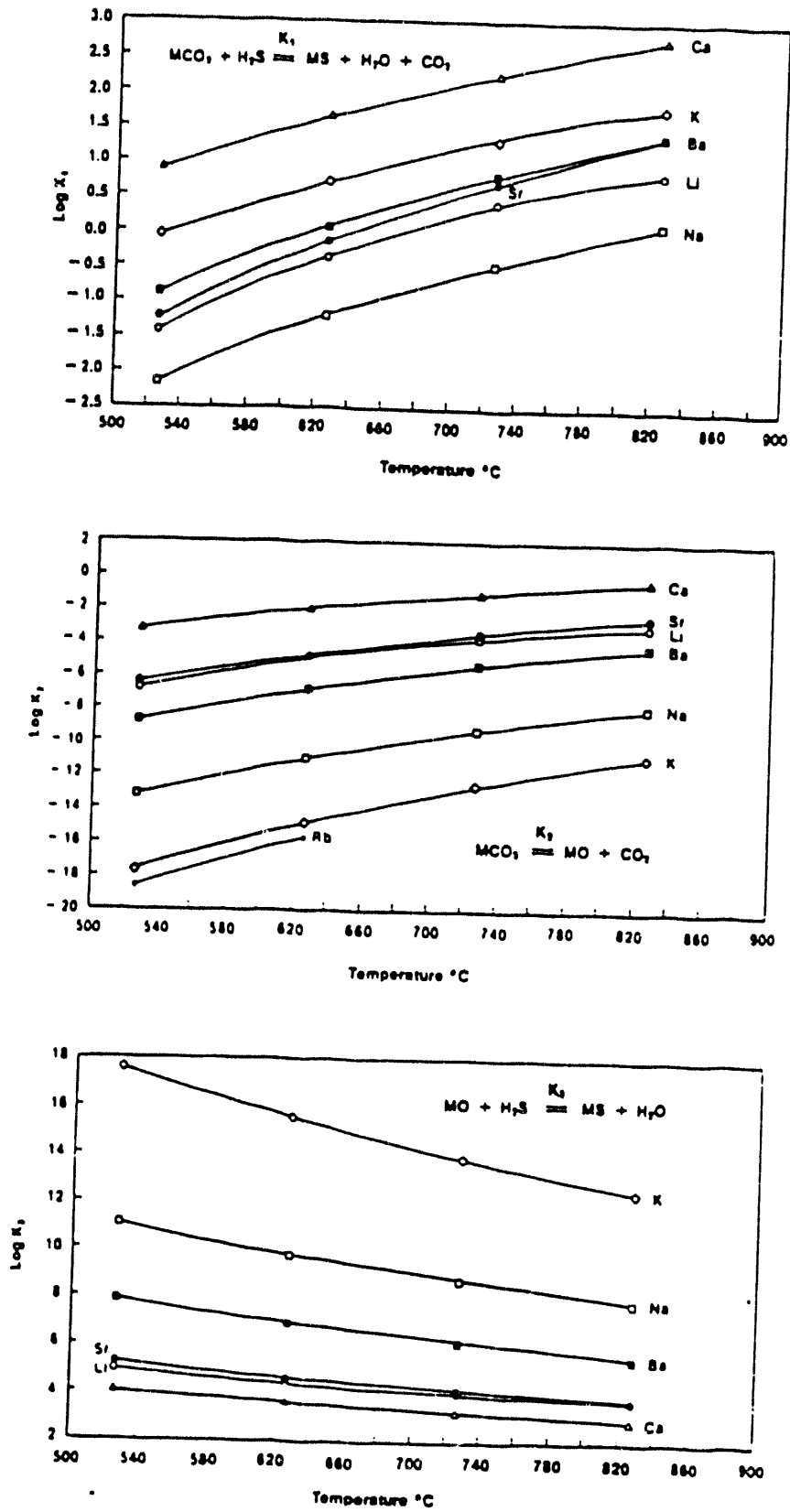


Figure 4.1. Log K versus temperature for reactions of pure carbonate salts. Top: $\log K_1$. Middle: $\log K_2$. Bottom: $\log K_3$

Table 4.2. Metal ion content of alkali and alkaline earth carbonate salts.

Salt	Metal ion content, weight percent		
	<u>theoretical</u>	<u>observed</u>	
		as received	after heating
Li ₂ CO ₃	18.78	16.37	18.69
Na ₂ CO ₃	43.38	38.82	43.75
K ₂ CO ₃	56.58	52.47	57.96
Rb ₂ CO ₃	74.02	68.18	nd
Cs ₂ CO ₃	81.58	33.25	79.16
CaCO ₃	40.04	40.33	nd
SrCO ₃	59.35	61.36	nd
BaCO ₃	69.59	65.69	70.67

Thermal gravimetric analysis (TGA) was used to determine the water content of the various carbonate salts and, more importantly, to determine their stability with respect to oxide formation and their volatility. In general, TGA data was collected under an N₂ atmosphere or a CO₂ atmosphere. Samples were heated from 30 to 830°C at a rate of 40°C/min. The temperature was maintained at 830°C for 10 min prior to cooling to room temperature. In general, it was found that heating of as received salts under N₂ led to a weight loss at relatively low temperature attributable to desorption of bound water from the sample. This is illustrated, for example, by the TGA trace (Figure 4.2) of as received Na₂CO₃ which exhibits a 20.05% weight loss ending at 230°C. The heat treatment of carbonate salts described above generally reduced the water content of the salts to near zero. Again, this is illustrated by the TGA trace for Na₂CO₃ after heating (Figure 4.2) which shows no water desorption. Exceptions were the salts Rb₂CO₃ and Cs₂CO₃. The salts Rb₂CO₃ and Cs₂CO₃ were heated a second time as above. TGA traces of both salts after heating as above showed that bound water was still present, suggesting that these salts readily absorb water when handled even briefly in the air.

In addition to the relatively low temperature weight loss ascribed to water, a few of the carbonate salts exhibited a high temperature weight loss when heated under a N₂ atmosphere (Table 4.3). This can be assigned to loss of CO₂ via oxide formation as in reaction (2) above. With the exceptions noted below, a high temperature weight loss was not observed when salt samples were heated under flowing CO₂ (15 psia), which is consistent with the chemistry of reaction (2) and with the fact that most carbonate salts were nonvolatile to temperatures of 830°C.

Compared with the other salts, MgCO₃, La₂(CO₃)₃, and Eu₂(CO₃)₃ are unusual. MgCO₃¹⁴ heated under N₂ or CO₂ exhibited the same TGA trace, which was characterized by a continuous weight loss over the entire heating range. The rare earth carbonates La₂(CO₃)₃ and Eu₂(CO₃)₃ apparently decompose to oxides in the presence or absence of CO₂ (Figures 4.3 and 4.4). Under N₂, both salts exhibited two high temperature weight losses beginning at 430 and at 650°C. Under CO₂, La₂(CO₃)₃ exhibited one weight loss starting at 470°C while Eu₂(CO₃)₃ exhibited two at 490°C and 690°C.

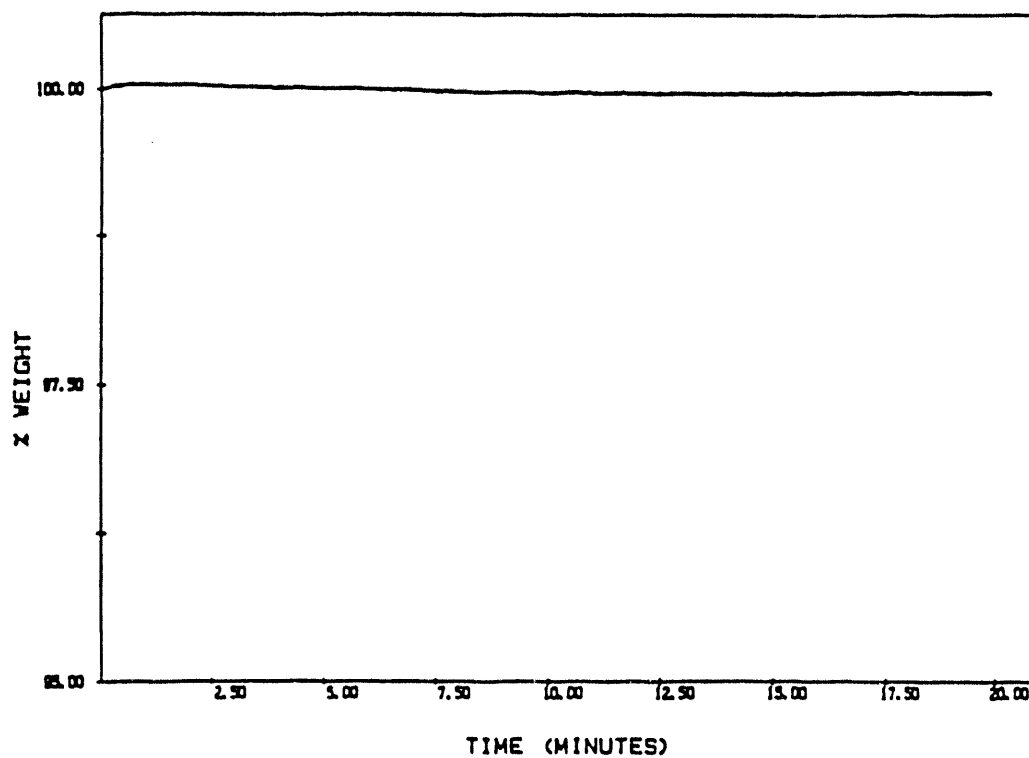
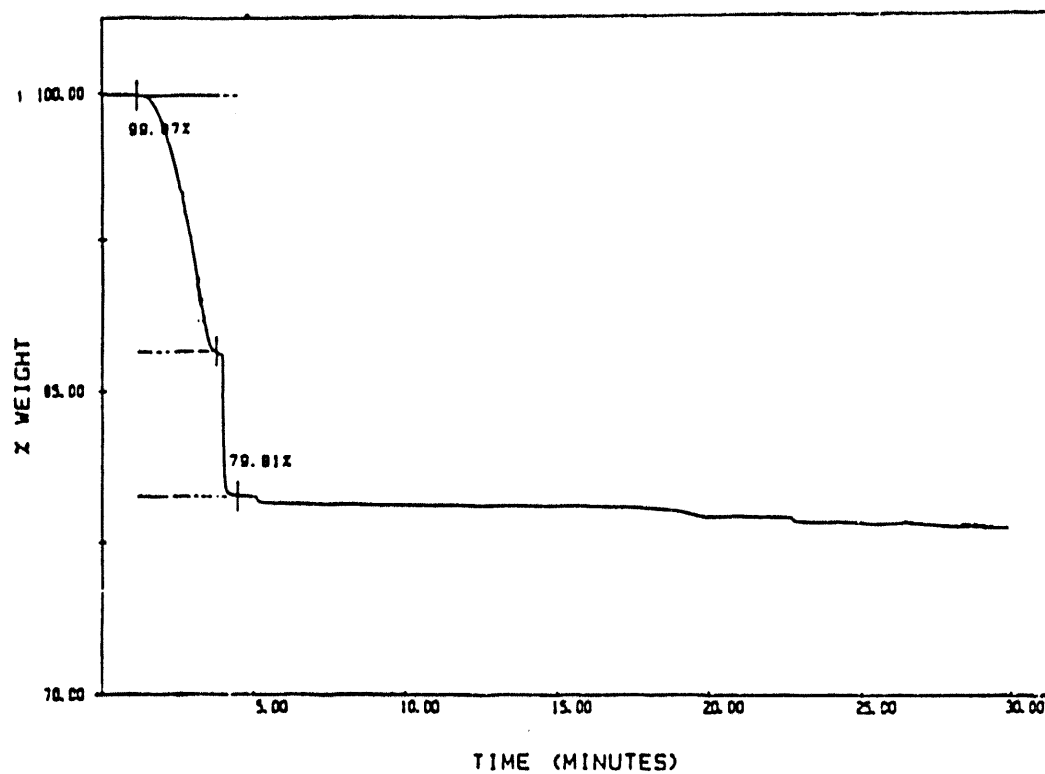


Figure 4.2 TGA traces of Na_2CO_3 obtained upon heating under a N_2 atmosphere.
 30°C to 830°C at 40°C/min.
 Top: As received salt.
 Bottom: After heating under a CO_2 atmosphere.

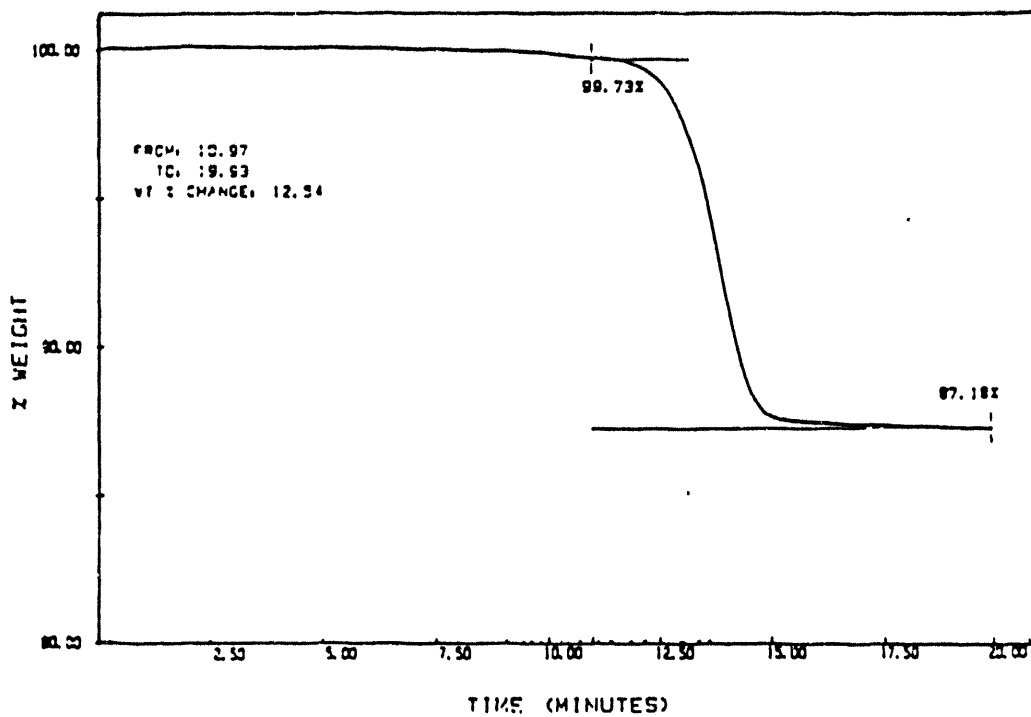
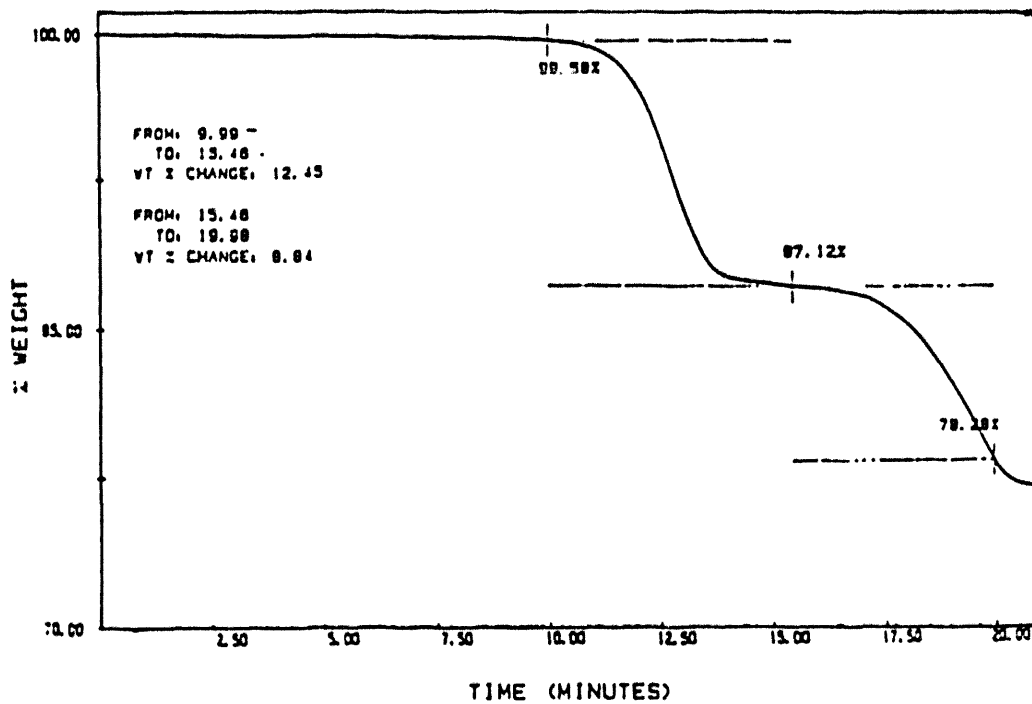


Figure 4.3 TGA traces of $\text{La}_2(\text{CO}_3)_3$.
 30°C to 830°C at 40°C/min.
 Top: Sample heated under a N_2 atmosphere.
 Bottom: Sample heated under a CO_2 atmosphere.

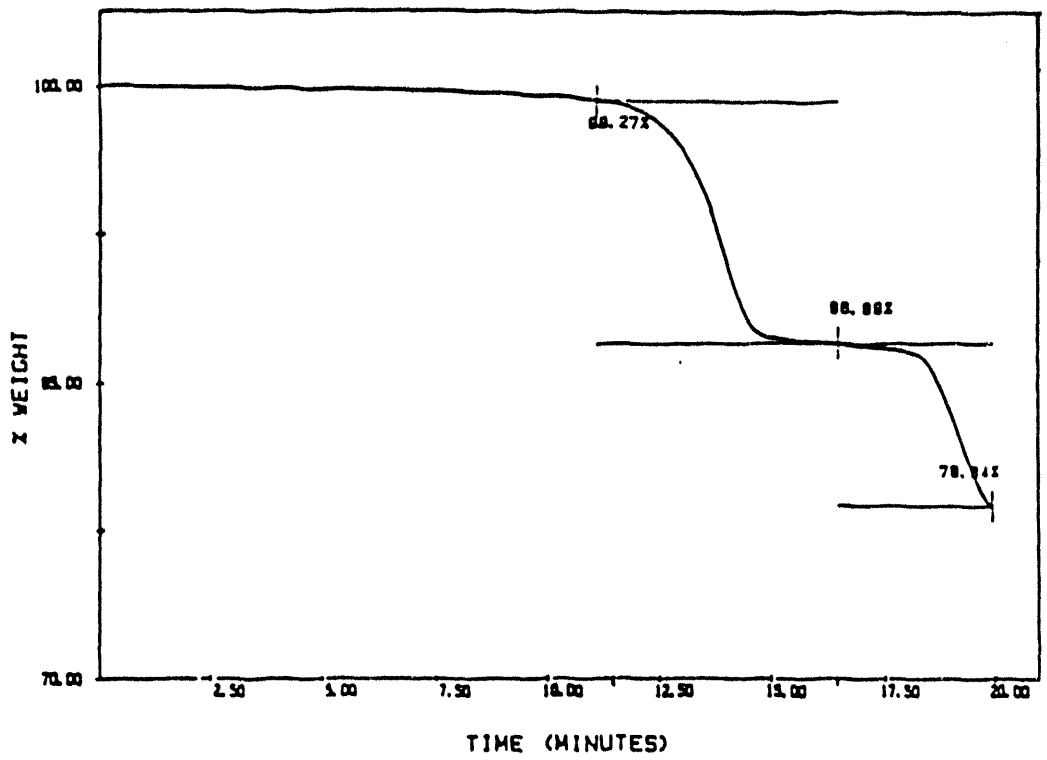
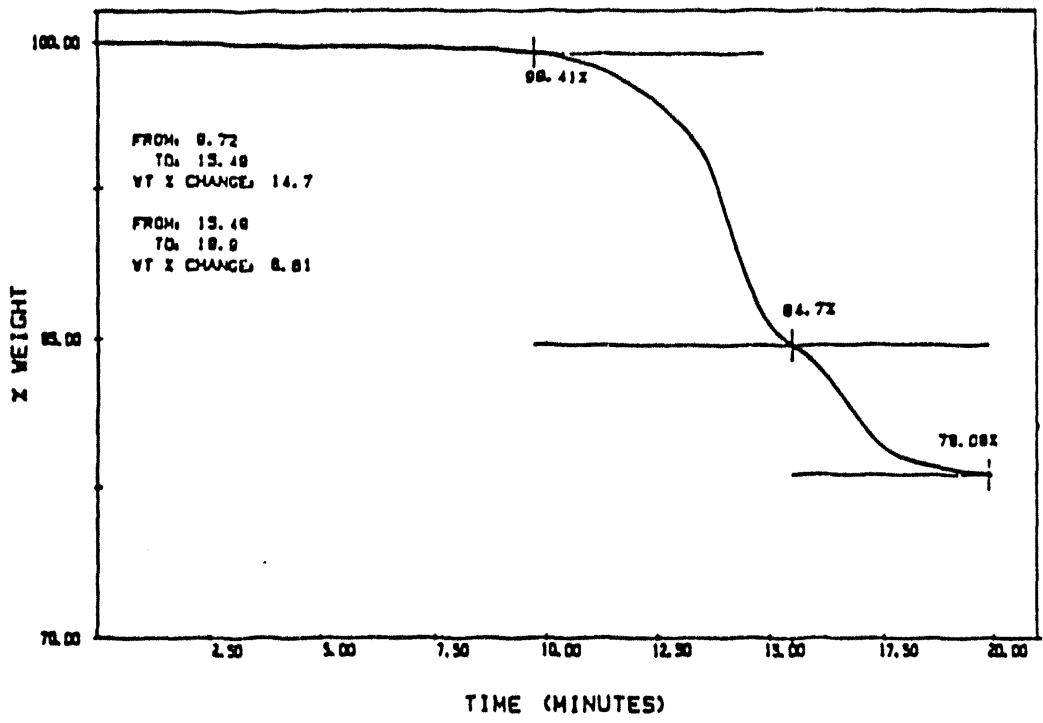


Figure 4.4 TGA traces of $\text{Eu}_2(\text{CO}_3)_3$.
 30°C to 830°C at 40°C/min.
 Top: Sample heated under a N_2 atmosphere.
 Bottom: Sample heated under a CO_2 atmosphere.

Carbonate salts were also characterized using differential thermal analysis (DTA). DTA data were most often collected under an N₂ atmosphere between 30 and 1000°C for as received salts and for salt after heat treatment. Table 4.4 summarizes the observed endotherm temperatures and a representative DTA trace is illustrated in Figure 4.5. For the as received samples, endotherms below 300°C correspond to desorption of bound water, consistent with the above TGA data. Higher temperature endotherms correspond either to melting or decomposition to the oxide and CO₂ as in reaction (2). For reference, literature melting points of various pure carbonates are listed in Table 4.4. Additional DTA information for pure carbonate salts is available in the literature.¹⁴ Endotherms for La₂(CO₃)₃ and Eu₂(CO₃)₃ are probably the result of decompositions to oxides since weight losses at comparable temperatures were observed in the TGA. Literature DTA results for La₂(CO₃)₃ show endotherms as 460°C and 915°C reportedly due to reactions 4 and 5 respectively:¹⁴



where La₂O₃•CO₂ is the mixed oxide-carbonate salt La₂O₂(CO₃).

Table 4.3. High temperature weight losses for pure carbonate salts.

Salt	under N ₂	under CO ₂
Li ₂ CO ₃	570	none
Na ₂ CO ₃	none	none
K ₂ CO ₃	none	none
Rb ₂ CO ₃	none	none
Cs ₂ CO ₃	none	none
MgCO ₃	continuous*	continuous*
CaCO ₃	650	none
SrCO ₃	590**	610**
BaCO ₃	none	none
La ₂ (CO ₃) ₃	430, 650	470
Eu ₂ (CO ₃) ₃	430, 650	490, 690

*continuous weight loss over entire temperature range, 30 - 830°C.

**relatively small weight loss, perhaps water.

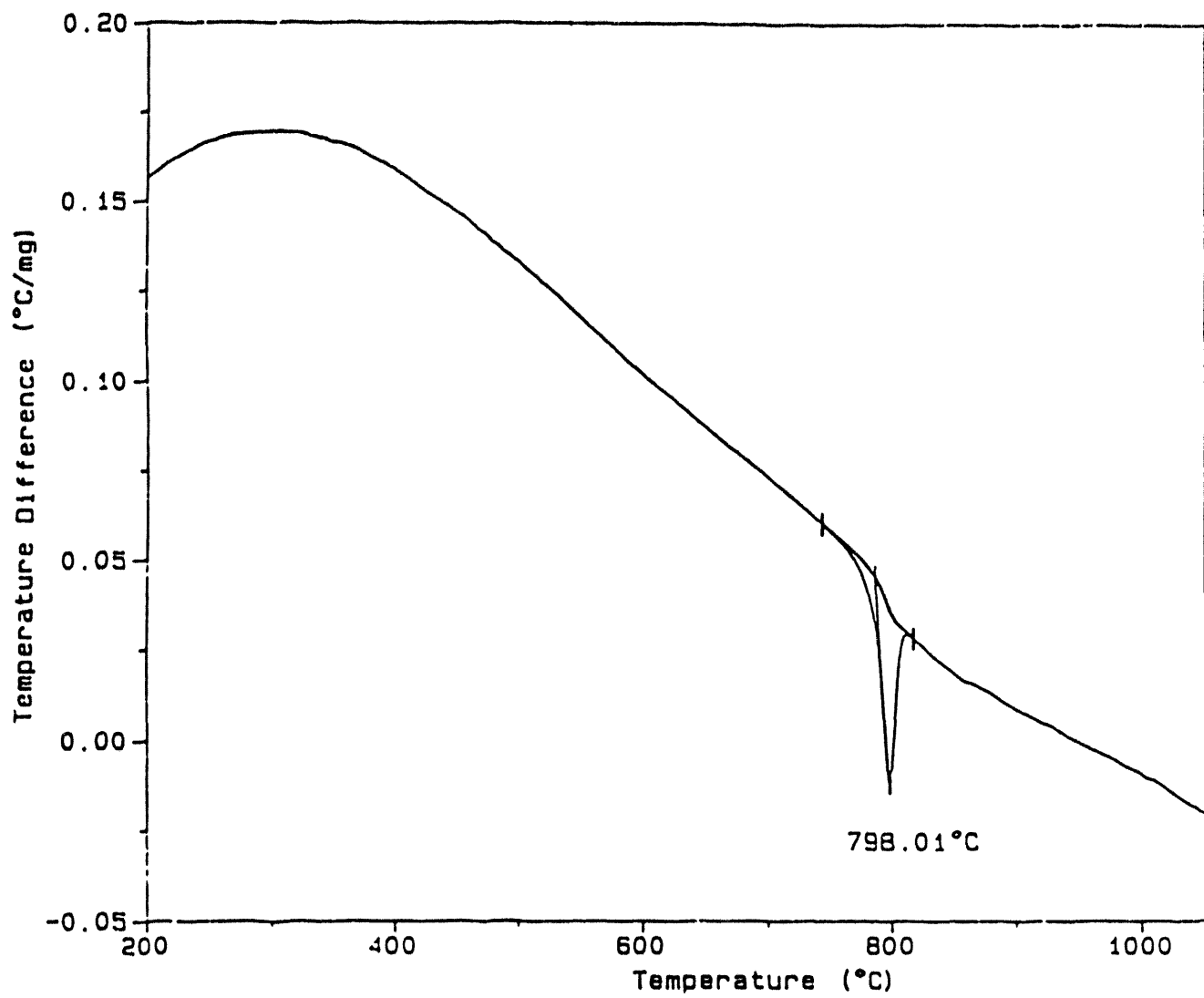


Figure 4.5 DTA trace of Cs_2CO_3 upon heating under a N_2 atmosphere.

Table 4.4. Endotherms for pure metal carbonate salts between 30 and 1000°C under a N₂ atmosphere.

Salt	Endotherm temperature, °C		lit. mp(°c) ^{a, 7,15}
	as received	after heating under CO ₂	
Li ₂ CO ₃	742	741	723
Na ₂ CO ₃	130, 849	459, 861	858
K ₂ CO ₃	147, 305, 896	785, 913	898
Rb ₂ CO ₃	509, 865	885	837
Cs ₂ CO ₃	105, 233, 785	798	-
MgCO ₃	283, 476	94, 340, 450	-
CaCO ₃	851	849	1339
SrCO ₃	937	936	1497
BaCO ₃	823	815	1740
La ₂ (CO ₃) ₃	not done	509, 776	-
Eu ₂ (CO ₃) ₃	not done	554, 660	-

a. some literature melting points were for salt at higher than ambient pressure

4.1.3. Preparation and characterization of carbonate mixtures.

A series of carbonate salt mixtures for subsequent evaluation in H₂S-selective membranes were prepared and characterized. Details concerning the preparation of these mixtures can be found in the Section 3.0. A typical procedure was as follows. Weighed quantities of the appropriate salts were ground into a mixture of fine powder using a mortar and pestle. The mixture was transferred to a gold crucible and heated under an atmosphere of CO₂ until it was molten, typically 550°C. Following rapid cooling to room temperature, the mixture was ground into a fine powder, dried at moderate temperatures under CO₂, and subsequently protected from atmospheric moisture.

The compositions of various mixtures prepared are listed in Table 4.5. The first of these, mixture 30-A, a ternary mixture of Li₂CO₃, K₂CO₃, and CaCO₃, was designated as the "base composition." The H₂S reactivity of this composition has been reported in the literature.⁹ Most of the other mixtures were prepared by addition of roughly 20 mole percent of a fourth carbonate to the base composition. One mixture, 40-1, was a ternary mixture which did not contain Li₂CO₃ and was prepared in an attempt to improve ceramic/carbonate salt compatibility. The literature has few references to low melting carbonate mixtures which do not contain Li⁺ and most of these have relatively high melting points, for example, 56 mole % Na₂CO₃/44 mole %K₂CO₃ which melts at 710°C.³ Mixture 40-1, which contained about equimolar quantities of Na₂CO₃, K₂CO₃, and Cs₂CO₃ was molten at 550°C. One additional quaternary mixture, 34-1, was prepared for which H₂S reactivity data is available.⁹

Table 4.5. Compositions and melting temperatures of carbonate mixtures prepared.

Components	Composition, mole %									
	30-A	34-1	27-1	23-2	31-1	32-1	34-2	25-2	26-1	40-1
Li ₂ CO ₃	49.0	37.36	35.29	32.98	32.87	33.27	35.34	34.67	36.42	
K ₂ CO ₃	25.2	19.26	21.82	22.38	22.22	22.40	21.74	22.19	22.59	33.23
CaCO ₃	25.7	20.06	23.71	25.06	25.01	24.73	23.69	23.42	22.81	
Na ₂ CO ₃		23.30								33.09
Rb ₂ CO ₃			19.59							
Cs ₂ CO ₃				19.19						33.68
SrCO ₃					19.89					
BaCO ₃						19.60				
MnCO ₃							19.23			
La ₂ (CO ₃) ₃								19.72		
Eu ₂ (CO ₃) ₃									18.18	
MP(°C)	485	405, 449	447, 482	426, 443	481, 482	469, 443	*	*	*	429, 546

* Unstable at or below melting point

The melting points of the various carbonates mixtures, as determined by DTA and described in more detail below, are also listed in Table 4.5. Three of the mixtures were found to be unstable at or below their melting points. One of these, mixture 34-2, contained Mn(II)CO₃ in an attempt to produce a transition metal containing melt. Heating of this mixture to 550°C resulted in a deep brown/red liquid which appeared to evolve gas. Subsequently, a literature reference¹⁶ was found which reported that MnCO₃ is unstable in a Li₂CO₃-Na₂CO₃-K₂CO₃ eutectic above 400°C and that CO₂ and CO are liberated as in reaction (6):



This points out the potential difficulty using metal ions with more than one readily accessible oxidation state to prepare molten carbonate mixtures.

Also unsuccessful were attempts to prepare carbonate mixtures containing the rare earth elements La(III) and Eu(III). Heating of mixtures 25-2 (La) and 26-1 (Eu) to 550°C and subsequently to 600°C did not result in a molten product. After cooling to room temperature under CO₂, it was determined that the mixtures had lost 7.1% (25-2) and 54.1% (26-1) of their initial weights, implying decomposition of significant quantities of salt to oxides. This can be traced to the instability of La₂(CO₃)₃ and Eu₂(CO₃)₃ even in the presence of CO₂ as demonstrated by the TGA data for the pure salts (see above). The thermal instability of these two salts makes their use in H₂S selective membranes unlikely.

TGA data for carbonate salt mixtures were obtained at temperatures of 30 to 830°C. As for the pure salts, some carbonate mixtures exhibited relatively low temperature, below

400°C, weight losses attributable to desorption of bound water. High temperature weight losses were observed when mixtures were heated under N₂ (Table 4.6). These losses correspond to decomposition of some carbonate to oxide (reaction (2)). Decomposition to the oxide was largely eliminated when the various mixtures were heated under CO₂ and high temperature weight losses were generally not observed (see Table 4.6). Results of additional TGA experiments at elevated temperatures demonstrated that carbonate salt mixtures were largely nonvolatile under a CO₂ atmosphere. A sample of the base composition (30-A) under CO₂ showed no change in the sample weight after 5.5 hours at 650°C. Similarly, the Cs⁺ containing mixture 27-1 showed no weight loss under CO₂ when held at 550°C for 110 min.

The melting points of the carbonate salt mixtures were of particular importance since these must fall within the range of temperatures amenable to membrane testing, 400 to 800°C. As shown above for pure salts, DTA is particularly useful in this regard. DTA data, which is summarized in Tables 4.7 and 4.8, were obtained for the mixtures under a N₂ and/or CO₂ atmospheres at between 30 to 1000°C. Representative of the DTA traces for the various mixtures are provided for mixture 30-A in Figure 4.6.

Table 4.6. TGA results for carbonate salt mixtures. High temperature weight losses for mixtures under N₂ or CO₂ atmospheres.

Mixture	metal ions present ^a	T(°C) of weight loss	
		under N ₂	under CO ₂
30-A	Li, K, Ca	700	none
34-1	Li, K, Ca, Na	675	none
23-2	Li, K, Ca, Rb	700	none
27-1	Li, K, Ca, Cs	640	none
31-1	Li, K, Ca, Sr	660	730*
32-1	Li, K, Ca, Ba	630	none**
40-1	K, Na, Cs	720	800*

a. Refer to Table 4.5 for exact compositions.

* very slight weight loss

** slight weight increase beginning at 510°C

Each mixture exhibited one or more endotherms below 550°C which can reasonably be attributed to melting. This assignment is supported by the similarity of the endotherm temperature for a mixture obtained under N₂ and CO₂. Further, the absence of weight loss in the TGA below 550°C imply that these endotherm are not the result of sample decomposition. For two samples under CO₂, 30-A and 40-1, an endotherm at higher temperatures, 895°C and 738°C respectively, may result from slight decomposition to oxide. Low temperature endotherms, less than 400°C, attributable to desorption of bound water, were not observed, with the exception of sample 40-1, implying that the mixtures were anhydrous. Some samples exhibit exotherms at temperatures below 400°C (Table 4.8) which are most reasonably assigned to a crystallization process.

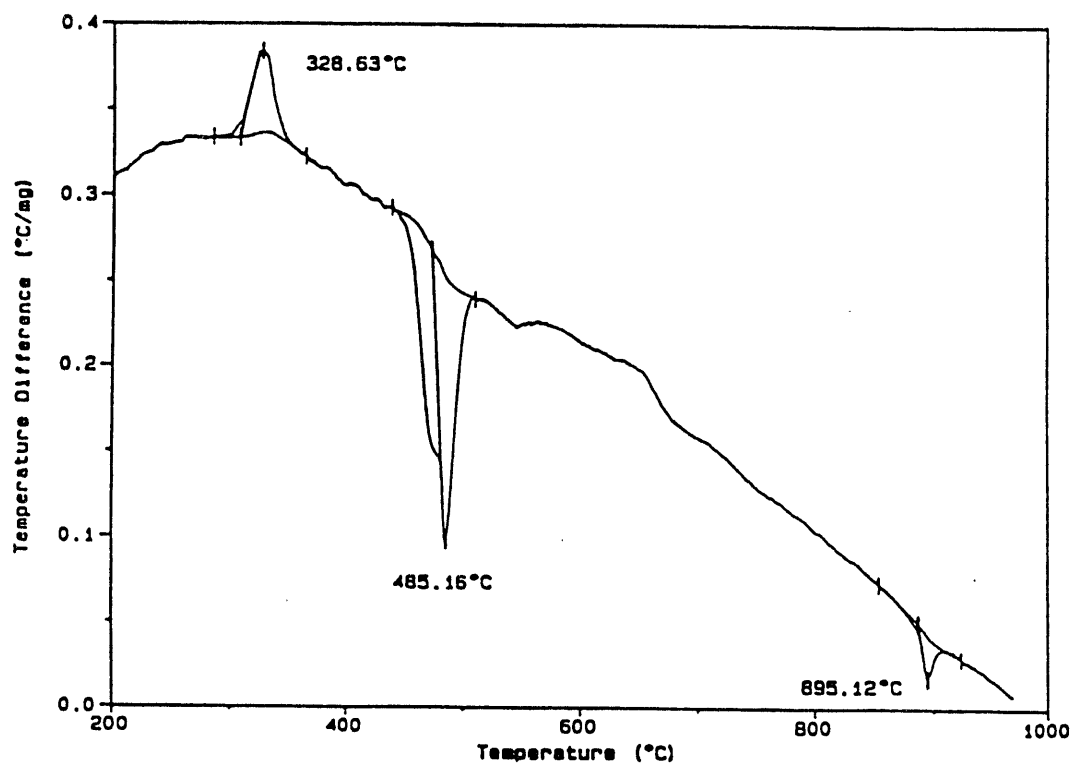
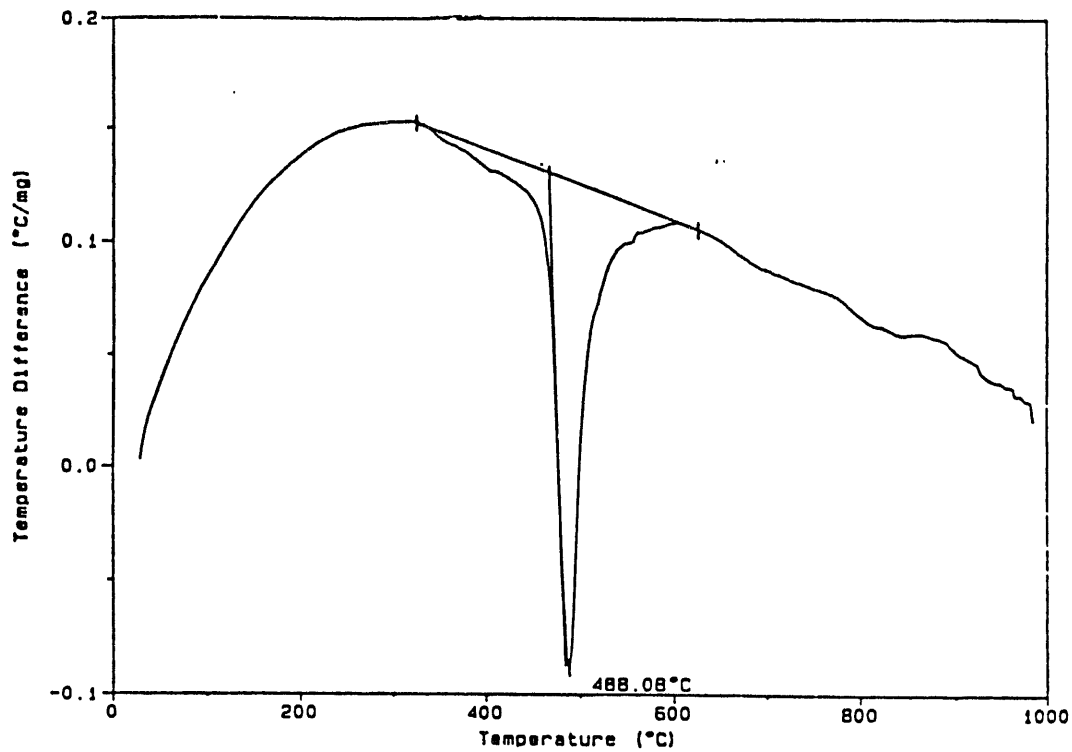


Figure 4.6 DTA traces of the base composition carbonate mixture 30-A.
 Top: Sample heated under a N_2 atmosphere.
 Bottom: Sample heated under a CO_2 atmosphere.

Table 4.7. DTA results for carbonate mixtures. Observed endotherm temperatures between 30 and 1000°C for samples under N₂ or CO₂ atmospheres.

Mixture	metal ions present	Endotherm T (°C)	
		under N ₂	under CO ₂
30-A	Li, K, Ca	488	485, 895
34-1	Li, K, Ca, Na	405, 459	405, 449
23-2	Li, K, Ca, Rb	456, 491	447, 482
27-1	Li, K, Ca, Cs	433, 457	426, 443
31-1	Li, K, Ca, Sr	483	481
32-1	Li, K, Ca, Ba	470	469
40-1	K, Na, Cs	-	247, 426, 551, 738

Table 4.8. DTA results for carbonate mixtures. Observed exotherm temperatures between 30 and 1000°C for sample under N₂ or CO₂ atmospheres.

Mixture	metal ions present	Exotherm T (°C)	
		under N ₂	under CO ₂
30-A	Li, K, Ca	-	329
34-1	Li, K, Ca, Na	332	332
23-2	Li, K, Ca, Rb	-	-
27-1	Li, K, Ca, Cs	-	-
31-1	Li, K, Ca, Sr	394	390
32-1	Li, K, Ca, Ba	357	355
40-1	K, Na, Cs	-	-

4.1.4. Preparation and characterization of sulfide-containing carbonate mixtures.

Little literature data is available concerning the melting points of carbonate salt mixtures containing added sulfide ions.¹⁷ Therefore, to mimic the salt compositions that might be expected upon exposure to H₂S and to determine the melting points of these compositions, a series of carbonate mixtures containing added sulfide ion were prepared. Sulfide ion was added to the base composition 30-A by replacing some CaCO₃ with CaS. The sulfide ion content ranged from 5 to 25 mol percent. Compositions are listed in Table 4.9. Each sample was contaminated with colored impurities along with a gold colored solid believed to be iron sulfide (see Section 3.0 for details).

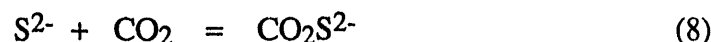
DTA results for sulfide-containing salt mixtures are listed in Table 4.10. Samples were heated from 30 to 1000°C under a CO₂ atmosphere. Each mixture exhibited one or two endotherms below 550°C which can be attributed to melting. That sulfide-containing carbonate mixtures are liquids at reasonable temperatures is critical to the success of molten carbonate membranes for removal of H₂S. Partial solidification of the melt during membrane operation could lead to membrane failure. DTA data suggest that,

even at sulfide ion concentrations as high as 25 mole percent, the base composition mixture will remain molten at a reasonable minimum temperature of 600°C.

Two of the mixtures listed in Table 4.9, 38-1 and 38-2, were characterized by TGA. Samples were heated under CO₂ from 30 to 830°C which resulted in a slight weight increase beginning at about 325°C and totaling about 0.9 weight percent by 830°C. The weight increase presumably corresponds to reaction of CO₂ and trace water with sulfide in the melts as in reaction (7):



or by reaction of CO₂ with the sulfide as in reaction (8):¹⁸



Subsequent reaction with additional CO₂ to COS and carbonate, as in reaction (9), is reasonable:



It should be noted that the above sulfide containing melts most likely contained some sulfate in addition to sulfide. The infrared (IR) spectra of the mixtures listed in Table 4.9 were obtained as KBr pellets. Each exhibited bands in addition to those expected for carbonate. The IR spectrum of the base carbonate mixture 30-A containing no added sulfide exhibited bands at 1480, 1420, 868, 713 and 496 cm⁻¹. In contrast, the spectrum of mixture 46-2 which contained 24.69 mole % sulfide exhibited the above bands and additional bands at 1265, 1113, 1091, 619, and 488 cm⁻¹. At least two of these bands, 1113 and 619 cm⁻¹, can be assigned to free sulfate¹⁹ which exhibits bands at 1104(vs) and 613(s) cm⁻¹. The spectra of the other sulfide ion containing mixtures had similar bands. The IR spectrum of the CaS used for sample preparation was featureless and eliminated it as a source of sulfate. The most likely source is air oxidation of sulfide either during heating of the mixture under flowing CO₂ or during the rapid cooling of the hot mixture, which was done in air.

Table 4.9. Composition of carbonate salt mixtures containing added sulfide ion.

Salt	Composition, mole %				
	38-1	46-1	38-2	43-1	46-2
Li ₂ CO ₃	49.02	49.11	48.34	49.35	50.90
K ₂ CO ₃	25.32	24.96	24.93	25.88	24.40
CaCO ₃	20.67	15.13	15.57	-	-
CaS	5.00	10.80	11.16	24.77	24.69

Table 4.10 DTA exotherm and endotherm temperatures for sulfide ion containing carbonate mixtures.

Mixture ^a	mole % CaS present	Exotherm, T(°C)	Endotherm, T(°C)
38-1	5.00	342, 914	489
38-2	11.16	356	479, 528
46-1	10.80	356	477, 550
46-2	24.69	368	474, 545

a. See Table 4.9 for exact compositions.

4.1.5. Determination of equilibrium constants for reaction of H₂S with molten carbonate mixtures.

To carry out the experiments necessary to obtain equilibrium constant values for reaction (1), a test facility to determine the H₂S absorption properties of carbonate salt mixtures under IGCC conditions was designed and constructed. This facility was also equipped to determine the permselective properties of molten carbonate membranes as described in a subsequent section. Because of the high temperatures and pressures of operation and the use of toxic and reactive gases, the test facility was designed for remote operation and was housed in a process development cell.

The facility consisted of three units which are illustrated schematically in Figure 3.1: a gas supply unit, an absorption unit and a membrane test unit. The gas supply unit consisted of a gas manifold and two gas mixing vessels. Each mixing vessel was equipped with a paddle-type stirrer to insure well blended mixtures. Water vapor was obtained by addition of liquid water to the mixing vessel and heating to complete vaporization, while other gases were added by pressure. Gas mixtures were analyzed by gas chromatography (GC) prior to use.

The absorption unit consisted of a reactor and dosing and sampling volumes. The reactor was a high pressure and temperature stainless steel Parr reactor. The inside wall of the reactor was insulated with an alumina liner, which was lined in turn with a gold vessel. The carbonate melt to be examined was contained in the gold vessel. The dosing volume was used to supply a known quantity of a gas mixture to the reactor, and the sampling volume was used to remove a portion of the gas above the melt for analysis by GC.

Detailed procedures for conducting absorption experiments are in Section 3.2. A summary of a typical procedure follows. In one of the mixing vessels, an H₂S containing feed gas mixture was prepared and analyzed by GC. A weighed quantity of the carbonate mixture was added to the absorption vessel and gradually heated to the operating temperature, usually 560°C. A quantity of feed gas was transferred into the dosing volume. The molten salt was then exposed to a known quantity of the feed gas mixture delivered from the dosing volume. Once equilibrium was attained, a portion of the gas above the salt was withdrawn into the sampling volume and analyzed by GC. As described below, a knowledge of pressures and the composition of the gas phase at

equilibrium along with the quantity of H₂S absorbed permitted calculation of an equilibrium constant. **Minimum** errors of 1.5% are associated with the determination of molar quantities of gases (see Section 3.2 for details).

Excluding the cations for simplicity, reaction (1) can be rewritten as reaction (10):



The equilibrium constant for reaction (10), K, is given by the expression:

$$K = \frac{P_{\text{H}_2\text{O}} P_{\text{CO}_2}}{P_{\text{H}_2\text{S}}} \cdot \frac{[\text{S}^{2-}]}{[\text{CO}_3^{2-}]} \quad (11)$$

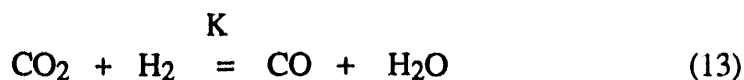
where P_i are partial pressures and [X] are molar concentrations. Equation (11) can be simplified to equation (12):

$$K = P \cdot \frac{x_{\text{H}_2\text{O}} x_{\text{CO}_2}}{x_{\text{H}_2\text{S}}} \cdot \frac{n(\text{S}^{2-})}{n(\text{CO}_3^{2-})} \quad (12)$$

where x_i are mole fractions, n_i are moles and P is the total pressure. Thus, calculation of K, requires a knowledge of the equilibrium mole fractions of CO₂, H₂O, and H₂S and the amount of H₂S absorbed by the melt.

Although the above experimental procedure in principle may appear straightforward, several significant problems made determination of accurate equilibrium constants very difficult. These included gas phase reactivity at high temperatures, quantification of gaseous water, and, more critically, H₂S-metal reactivity. These issues are addressed below.

4.1.5.1 Gas phase reactivity. A "blank" experiment, in which no salt was present, clearly indicated that feed gas mixtures were reactive at elevated temperatures. The absorption vessel containing a mixture of 32.1% CO₂, 46.5% H₂, and 21.4% CH₄ at 111.9 psia was heated to 550°C. After standing overnight, the pressure dropped slightly to 107.0 psia. GC analysis of the gas phase revealed the presence of CO in addition to the three original gases. Assuming that no other gases were present in the headspace,²⁰ individual concentrations were: 20.9% CO; 16.5% CO₂; 40.0% H₂; 22.6% CH₄. That the pressure in the absorption vessel remained nearly constant suggests that elemental carbon was not formed. In fact, when the absorption vessel was opened, no black residue was observed. It is reasonable to postulate that CO arises from the water gas shift reaction (13):



The value of K at 527°C calculated from literature data^{13,21} is 0.237. The above experimental partial pressures of CO₂, H₂, and CO, coupled with the assumption that the concentration of water and of CO were identical, result in a value of K of 0.66. Considering the crudity of the experiment, agreement between the calculated and experimental values of K are sufficient to imply the presence of water gas shift chemistry. In addition, it should be noted that various metal oxides, particularly those of iron, copper, cobalt, and molybdenum, have been shown to catalyze the water gas shift reaction, and at least for one particular catalyst, the presence of Cs₂CO₃ or K₂CO₃ led to enhanced catalytic activity.²¹ Such conditions might be encountered in a typical absorption experiment.

Observation of such gas phase reactivity prompted a consideration of other possible gas phase reactions. Table 4.11 lists some equilibrium constants calculated from literature thermodynamic data¹³ for such gas phase reactions over the temperature range of 527°C to 827°C.

Table 4.11. Equilibrium constant values for gas phase reactions.¹³

Reaction ^a	527°C	627°C	727°C	827°C
(a) CO ₂ + H ₂ = H ₂ O + CO	0.237	0.437	0.701	1.026
(b) CO ₂ + H ₂ S = COS + H ₂ O	0.0126	0.0213	0.0323	0.0455
(c) CO ₂ + CH ₄ = 2CO + 2H ₂	0.0069	0.542	17.86	313.0
(d) CO + H ₂ = C + H ₂ O	24.03	2.478	0.400	0.0901
(e) 2CO = C + CO ₂	101.5	5.666	0.571	0.0878
(f) CH ₄ + H ₂ O = CO + H ₂	0.0293	1.240	25.45	305.0
(g) H ₂ S + CO = COS + H ₂	0.053	0.049	0.046	0.044
(h) CO + 3H ₂ = CH ₄ + H ₂ O	34	1.24	0.0398	0.00334
(i) 2CO + 2H ₂ = CO ₂ + CH ₄	141	1.84	0.0566	0.00326

a: All species are gases, except C which is a solid.

At the lowest temperatures at which absorption experiments would be run, 560°C, other than reaction (a), only reactions (d) and (e) occur to an appreciable extent. However, at higher temperatures reactions (c) and (f) involving CH₄ become favorable. The gas phase reactivity of CO₂ with H₂S forming COS (reaction b) is relatively unfavorable over the temperature range of 527 to 827°C. The CH₄ forming reactions are thermodynamically favorable at lower than 527°C but become unfavorable at higher temperatures. The potential variety of reactions, of course, complicates analysis of absorption data.

4.1.5.2 H₂S absorption experiments. A series of absorption experiments involving the base composition carbonate mixture 30-A and H₂S containing feed gases were performed. Details of these experiments can be found in the Section 3.0. In the first experiment, 12666-2, the base composition carbonate mixture 30-A at 560°C was

exposed to a gas mixture containing 10.7% H₂S, 6.40% CO₂, 81.1% CH₄, and 1.8% H₂. Once equilibrium was achieved, GC analysis of the headspace gases revealed the presence and concentrations of CO and COS in addition to H₂S, CO₂, H₂ and CH₄ as listed in Table 4.12. The quantity of water in the gas phase was calculated by assuming that it was the difference between the sum of the above gases and the total quantity of gas present at equilibrium.

Table 4.12. Headspace analysis of gases at equilibrium in absorption experiment 12666-2

gas	concentration in	
	ppm	mole fraction
H ₂ S	80.8	9.608x10 ⁻⁴
CO ₂	2,678	3.185x10 ⁻²
CH ₄	64,665	7.692x10 ⁻¹
CO	7,567	8.998x10 ⁻²
COS	8.3	9.809x10 ⁻⁵
H ₂	5,941	7.065x10 ⁻²
H ₂ O	-	3.726x10 ⁻²

Using the above mole fractions of CO₂, H₂S, and H₂O and the calculated quantities of sulfide and carbonate ions present in the melt at equilibrium, a value of K₁ of 0.235 atm was obtained. Although to the best of our knowledge, literature data at 560°C is unavailable, the value of K₁ at 750°C for this salt mixture is 1.7 atm.⁹ Equilibrium constants for the reaction of interest increase with increasing temperature so that 0.2atm is a reasonable but perhaps somewhat high value for 560°C.

When the above run was completed, stirring of the melt was stopped and the absorption vessel was cooled to room temperature. Examination of the contents of the vessel revealed a black powder, presumed to be carbon, on the surface of a white solid. This observation implies that the black solid was generated upon cooling otherwise it would have been dispersed throughout the white solid phase. Such reactivity is consistent with the thermodynamics of carbon formation (see Table 4.11). In addition to the black solid, gold-colored solid deposits were observed on various metal surfaces, indicative of metal-H₂S reactivity. Energy dispersive X-ray spectroscopy (EDS) of deposits on the thermowells of the absorption vessel indicated the presence of the elements Fe, Ni, Cr, O, and S, consistent with the formation of metal sulfides. The identification of such deposits calls into question the value of K₁ obtained, since some of the H₂S thought to have been absorbed by the molten salt was actually consumed in formation of metal sulfides.

In a second absorption experiment, 12666-6, the base composition carbonate mixture at 560°C was exposed to a gas mixture containing 8.382% H₂S, 40.36% CO₂, 51.28% CH₄. At equilibrium, analysis of the headspace above the melt revealed the presence of CO, H₂, and COS in addition to H₂S, CO₂, and CH₄. Treating the absorption data as above resulted in an unrealistic value for the quantity of water vapor present at equilibrium and, thus, a value for the equilibrium constant could not be calculated. This points out the difficulty in determining relatively small amounts of water gas by difference. The sum

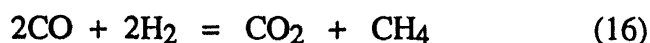
of the errors in the individual concentrations is likely to be large with respect to the concentration of water.

Absorption experiment 12666-15 involved 126.9 g of the base composition carbonate mixture 30-A at 560°C that was then exposed to a gas mixture consisting of 15.0% H₂S in CO₂. Although an inadvertent valve switch precluded a quantitative treatment, the data was qualitatively enlightening. After standing overnight, a portion of the headspace gases was withdrawn and analyzed by GC. Surprisingly, in addition to H₂S and CO₂, CO, H₂ and COS were detected. The ratio of gases with H₂S set equal to one were: H₂S, 1; CO₂, 43.0; CO, 9.2; COS, 0.045; H₂, 0.99. It is highly unlikely that H₂ resulted from reaction of H₂S with CO₂ (see Table 4.11 above). A more likely source of the observed H₂, and hence CO, is the oxidation-reduction reaction of H₂S with the non-gold metal components of the absorption vessel as in reaction (14):



Such consumption of H₂S makes the determination of an accurate equilibrium constant for the reaction of carbonate with H₂S quite difficult.

4.1.5.3 H₂S-metal reactivity. In an attempt to overcome the problems associated with the metal reactivity of H₂S, the various components of the absorption vessel were gold plated. Another absorption experiment, 12923-32, was performed using 125.8 g of the base carbonate mixture 30-A at 550°C. A feed gas containing only 0.5% H₂S in N₂ was dosed into the reactor and the system was allowed to come to equilibrium. A headspace analysis of the gas phase revealed the presence of CO₂, CH₄, CO, and H₂, but not H₂S or COS. Based on the assumption that no water is present in the gas phase, the gas concentrations at equilibrium were: CO₂, 2.82%; CO, 1.52%; CH₄, 1.24%; H₂, 1.30%. Such concentrations would appear to be unrealistically high considering that the feed gas contained only 0.5% H₂S. In any case, the presence of the above gases strongly implies that H₂ was formed by reaction of H₂S with metal. This was supported by visual examination after the run which revealed that much of the gold plating, especially on the thermowells, was no longer present. Some H₂S was apparently absorbed by the carbonate melt as well. This was the source of the CO₂ and H₂O (unobserved). CH₄ could arise from reaction of CO and H₂ as in reaction (15) and/or (16) below for which the calculated equilibrium constants at 527°C are relatively large (see also Table 4.11).



4.2 Ceramic Materials Development

The development of the porous ceramic membrane supports was broken down into a series of subtasks. Initially, a literature search was implemented to identify candidate

ceramic compounds. This search concentrated on the molten carbonate fuel cell literature. Candidate compounds identified via this search were then screened for chemical compatibility using a mixed powder screening protocol developed for this program. Those materials determined most suitable were then obtained in the form of dense coupons and the wetting behavior of the candidate salt mixtures was determined using a high temperature sessile drop test system. Containment strategies were then developed based on the observed wetting behavior. In conjunction with Golden Technologies, techniques were developed to produce the candidate ceramic materials in the form of porous disc membrane substrates with the desired pore size distribution. Methods were developed to impregnate these porous supports with the molten alkali carbonate salt mixtures identified in Section 4.1. These membranes were then submitted for membrane performance testing as described in Section 4.3.

4.2.1 Materials Selection

A literature survey was implemented, concentrating on the molten carbonate fuel cell (MCFC) literature. From this basis²²⁻²⁴ it was determined that silicon-based ceramics (SiC, Si₃N₄, SiO₂, etc.) react with molten carbonates to form low melting alkali silicates. Alumina, zirconia, and titania all react to form mixed oxides with the alkali from the carbonates, and MgO and CaO are soluble in the carbonate melts. However, AlN and TiB₂ are known to be stable in molten cryolite and some molten salts, spinel (MgAl₂O₄) is expected to be stable, and LiAlO₂ is known to be stable in MCFC environments; however, it is polymorphic and not used as a structural material. On this basis, in conjunction with discussions with Golden Technologies, five compounds were chosen for initial screening evaluation. Those were: titanium diboride (TiB₂), tungsten carbide (WC), calcium aluminate (CaAl₂O₄), magnesium aluminate (MgAl₂O₄), and aluminum nitride (AlN).

A series of experiments were performed to determine qualitatively the chemical compatibility of the selected ceramics with the base composition carbonate mixture 30-A (see Table 4.5). The experiments were performed by mixing a known weight of the ceramic powder with a 10:1 excess of the salt mixture in a gold crucible, placing the crucible in a furnace with a flowing CO₂ atmosphere, and heat treating the mixture for 24 hours at 600, 700, or 800°C. Results were evaluated by visual observation, weight change, and X-ray powder diffraction.

The TiB₂ was eliminated from further consideration due to excessive reaction with the molten salts. WC was observed to change color and to gain weight, indicating oxidation, and was also eliminated.

The weight loss results for CaAl₂O₄, MgAl₂O₄, and AlN are shown in Figure 4.7. Little or no weight loss was observed after the 24 hour heat treatment at 600°C. CaAl₂O₄ exhibited excessive weight loss (~98%) at 700 and 800°C. X-ray analysis indicated that the CaAl₂O₄ reacted at 700°C to form Ca₃Al₂O₆ and lithium aluminate (LiAlO₂) and at

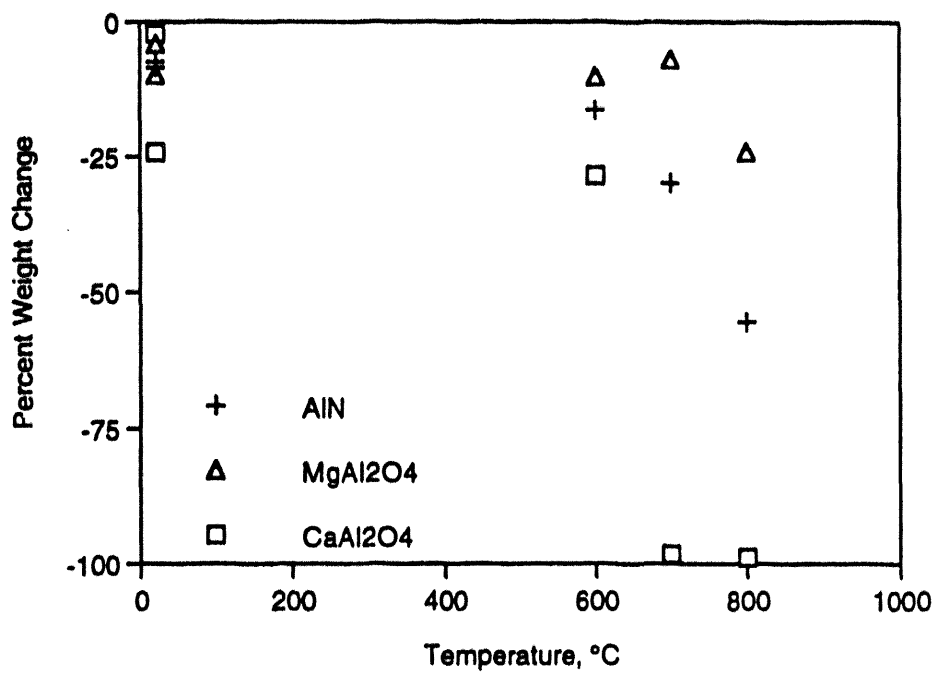


Figure 4.7 Weight loss of ceramic powders after 24 hour exposure to molten alkali carbonates

800°C to form LiAlO_2 and some $\text{Ca}_3\text{Al}_2\text{O}_6$. Based on these results CaAl_2O_4 was eliminated from further consideration. MgAl_2O_4 and AlN were observed to be more resistant to weight loss within the data scatter at 600 and 700°C. The AlN lost ~50% of its initial weight after salt exposure at 800°C while the MgAl_2O_4 lost ~20%. The X-ray analysis indicated that the AlN phase remained stable in contact with the molten salt while the MgAl_2O_4 at 800°C was converted to LiAlO_2 . Based on these results it was decided to continue evaluation of AlN and MgAl_2O_4 in wetting studies and to further investigate LiAlO_2 .

4.2.2. Wetting Behavior

Sessile drop experiments were conducted using the apparatus shown schematically in Figure 4.8. Contact angles are defined such that angles greater than 90° are considered non-wetting and angles less than 90° are considered wetting. AlN and MgAl_2O_4 samples were obtained from Golden Technologies in the form of dense plates which were cleaned in a two step procedure using chlorinated solvents. Tests were run in a tube furnace with a flowing CO_2 atmosphere. The hold time at temperature ranged from one-half to six hours. In addition, a series of long term tests was carried out with a maximum exposure time of 500 hours. A sessile drop test was also performed on gold to provide data needed to specify the desired pore size for fritted gold discs to be used, if needed, for initial membrane tests. The measured contact angle of the base composition carbonate mixture on gold was 52°.

Initial sessile drop experiments were performed using the molten salt composition listed above on samples of AlN previously obtained from a vendor other than Golden Technologies. In this case, a very low contact angle was observed (2-4°) indicating good wetting. Comparable wetting behavior was observed with the MgAl_2O_4 materials obtained from GTC with a measured contact angle of 6°. However, the contact angle measured with the same salt composition on the AlN material obtained from GTC was 130-134° indicating very poor wetting of the surface by the salt. Surface analysis of the two AlN materials using ESCA sputter depth profiling indicated that the surface of the GTC AlN was primarily composed of boron nitride as a consequence of the fact that the AlN plates were fired on BN setters. Table 4.13 compares the ESCA results for the two materials. Also included is the ESCA results for the GTC material after mechanically removing the BN surface layer using tumbling. When this BN surface layer was removed mechanically, the measured contact angle was 5-8°, in good agreement with the results from the other AlN material. It was further determined that a colloidal spray of BN applied to the surface of MgAl_2O_4 could result in an increase of the measured contact angle from 5-6° to 94-145°.

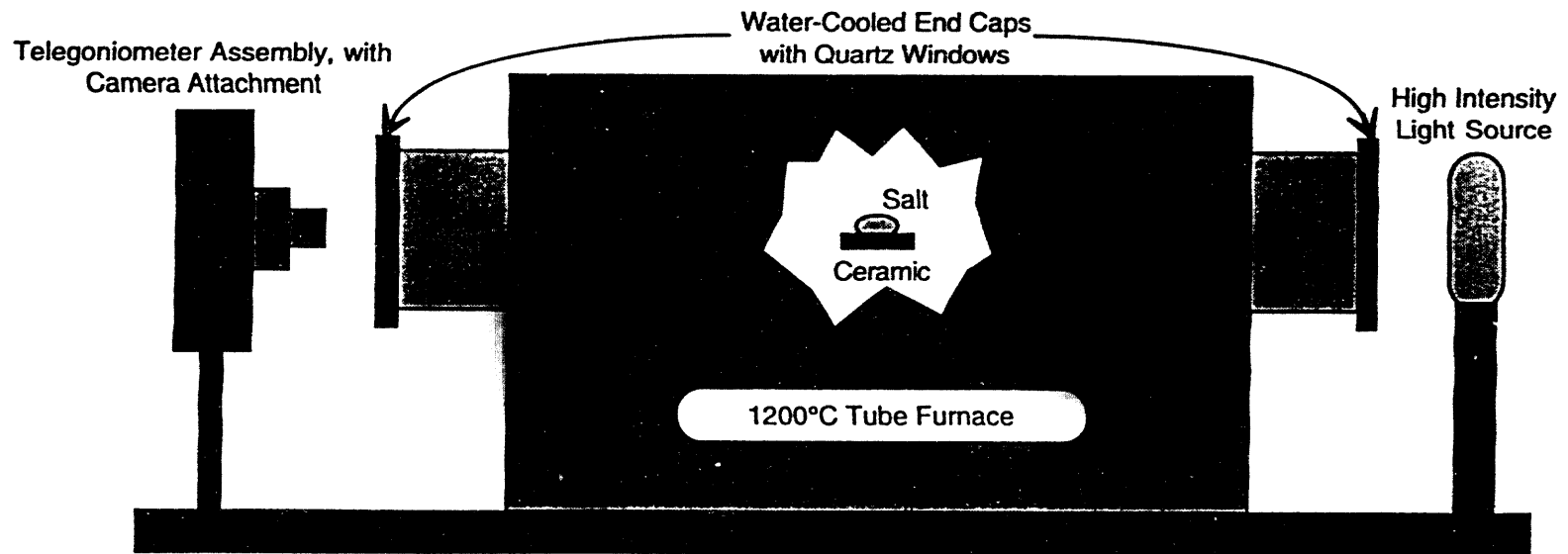


Figure 4.8 Sessile Drop Test System

Table 4.13. ESCA Surface Analysis of AlN Samples

Rel. Depth	TCL AlN		GTC AlN		GTC AlN (t)	
	B/N	Al/N	B/N	Al/N	B/N	Al/N
surface	-	1.1	0.53	0.09	-	1.03
cycle 1	-	1.4	0.54	0.08	-	0.94
cycle 2	-	1.5	0.51	0.08	-	0.84
cycle 3	-	0.81	0.46	0.20	-	0.78
cycle 4	-	0.81	0.45	0.20	-	0.82
cycle 5	-	0.89	0.49	0.30	-	0.86
cycle 6	-	0.86	0.46	0.35	-	0.85
cycle 7	-	0.89	0.42	0.38	-	0.90

The effect of the sulfide ion content of the salt melt on wetting of AlN (from GTC in the as-received condition) was also studied. Three S²⁻-containing salts were examined (see Table 4.9). The results are shown in Figure 4.9. As can be seen, the S²⁻ content has little effect except at the high (25%) level. In preliminary tests on MgAl₂O₄, the measured contact angles were 6° and 1° for the base mixture and the 11% S²⁻-containing mixture, respectively.

The results of long term tests of the wetting of AlN by sulfide ion containing salts are shown in Figure 4.10. In all cases, the contact angles are observed to decrease with exposure time. This could be the result of oxidation of the substrate, reaction between the salt and the substrate, or a combination of the two. Implications are that with time and contact with H₂S, the melt may creep.

4.2.3 Ceramic Substrate Development

Aluminum nitride and lithium aluminate were determined to be the best choices for further development as ceramic membrane supports. This determination was based on results from a series of initial screening experiments which indicated that AlN and LiAlO₂ were the ceramic materials with the best chemical stability in the presence of the molten mixed alkali carbonates. Work with MgAl₂O₄ was discontinued due to its reactivity with lithium containing salts at high temperatures as compared to AlN.

Wetting studies were used as a basis for the design of the desired microstructures for salt containment. This was particularly true in the case of AlN. It was not possible to obtain or fabricate dense samples of LiAlO₂ for use in wetting studies; however, it is known that LiAlO₂ is wet by the salt compositions of interest. In order to estimate the transmembrane pressure which the membrane could sustain without the loss of the salt, the capillary force equation was used:

$$\Delta P = 2 \gamma \cos \theta / r \quad (17)$$

where ΔP is the transmembrane pressure, γ is the surface tension of the molten salt, θ is the contact angle of the molten salt with the ceramic, and r is the radius of the pore in which the molten salt is immobilized. A typical value²³ of γ for a mixed alkali carbonate

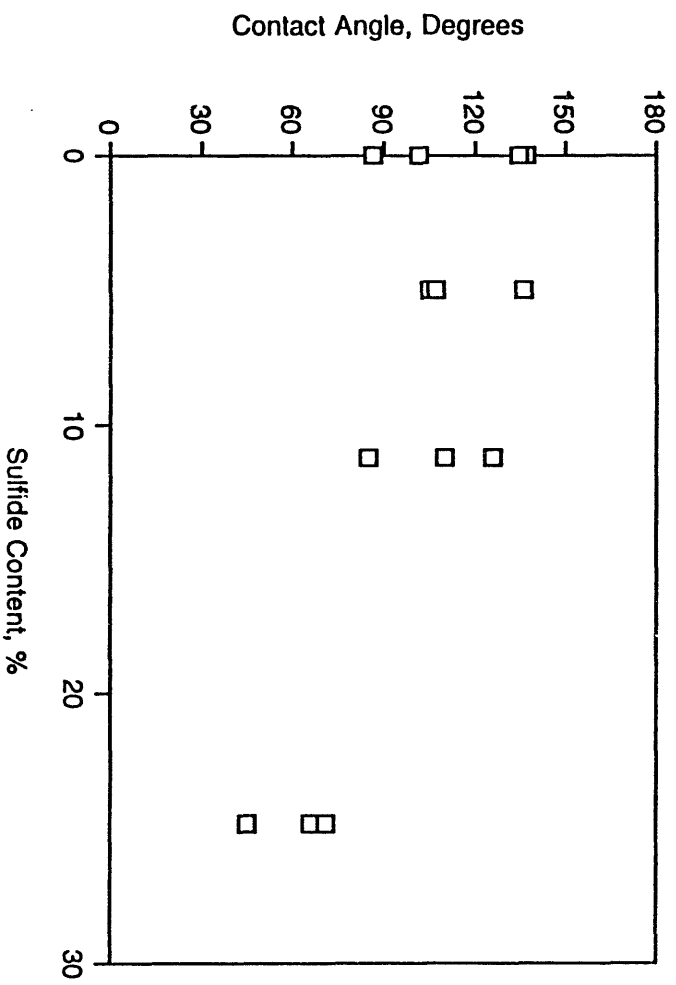


Figure 4.9 Effect of sulfide ion content of mixed alkali carbonates on the contact angle on AlN

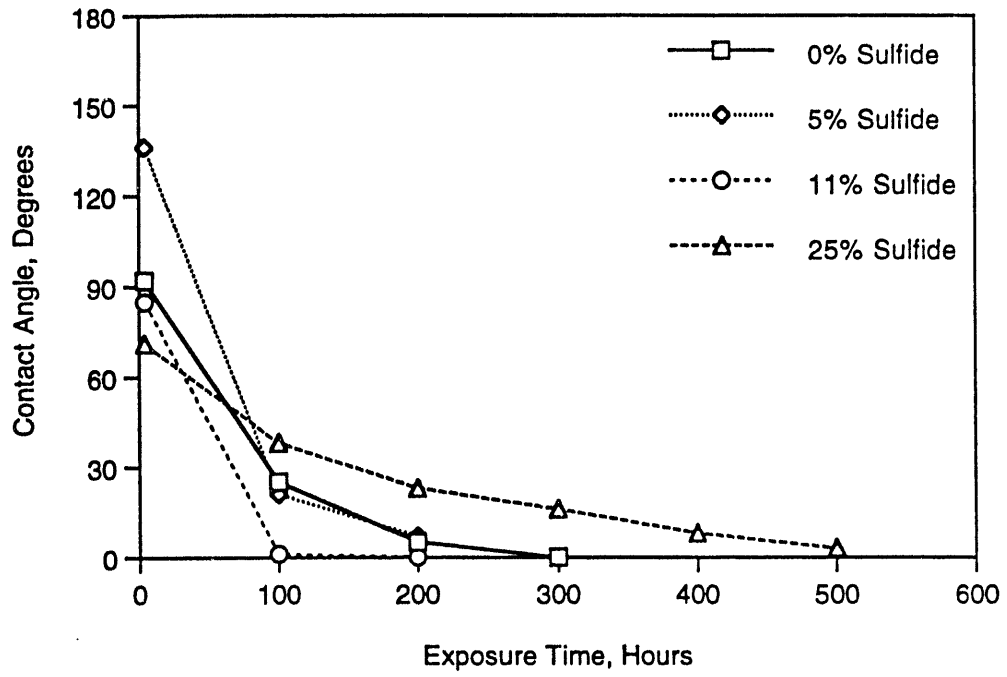


Figure 4.10 Effect of long term exposure on the contact angle of mixed alkali carbonates on AlN

at 600°C is ~225 mN/m and the contact angle for the salt on AlN is ~5°. Using these values and equation (17), the transmembrane pressure can be estimated as a function of membrane support pore radius. As can be seen in Table 4.14, at pore sizes less than 1 µm a significant pressure differential can be tolerated.

Table 4.14. Capillary Force as a Function of Support Pore Radius

Pore Radius, µm	ΔP, psi
0.1	653
1.0	65
5.0	13

GTC developed fabrication techniques to produce porous aluminum nitride. Using a standard starting aluminum nitride powder composition, GTC examined the effects of consolidation pressure and sintering temperature on pore size, pore size distribution, and pore volume fraction. In the case of material sintered at 1600°C, the porosity values ranged from a pore diameter of 0.58 µm with a pore volume fraction of 53.4% when consolidated at 2.5 kpsi to a pore diameter of 0.44 µm with a pore volume fraction of 45.1% when consolidated at 20 kpsi. For material fired at 1650°C, the values ranged from 0.6 µm/51.7% to 0.38 µm/42.3% for consolidation pressures of 2.5 to 20 kpsi. The fabrication conditions chosen to produce substrates for evaluation as membrane supports were 10 kpsi consolidation pressure fired at 1600°C and 2.5 kpsi consolidation pressure fired at 1650°C. These conditions resulted in membrane supports with a pore size of 0.34 µm with a pore volume fraction of 57.7% for the 1600/10 samples and a pore size of 0.52 µm with a pore volume fraction of 53.2% for the 1650/2.5 samples. Samples prepared using these process variables were infiltrated with the base composition carbonate mixture 30-A and used in experiments to evaluate the salt retention behavior of the supports as well as to produce supported salt membranes for membrane testing.

A similar fabrication study was undertaken at Air Products to develop porous lithium aluminate. Commercial lithium aluminate powders were mixed with an organic binder (polyethylene glycol) and a sintering aide (lithium fluoride). Initially, the level of binder and sintering aide were varied in an effort to fabricate dense lithium aluminate. When high density samples could not be produced, efforts were concentrated on fabricating material with controlled pore size. The early fabrication attempts resulted in samples consisting of primarily the higher alumina form of lithium aluminate (LiAl₅O₈) due to too high a firing temperature. These samples also had a bi-modal pore size distribution with pores at one and three microns diameter. Further refinement of the processing resulted in single phase LiAlO₂ with a narrow pore size distribution centered on ~3 µm. Results of the lithium aluminate fabrication study were transferred to GTC for continuation and production of membrane substrates.

Techniques, described in more detail in Section 3.3, were developed to infiltrate the molten carbonate salt mixtures into the porous aluminum nitride and lithium aluminate substrates. The long term salt retention behavior of these infiltrated substrates were then

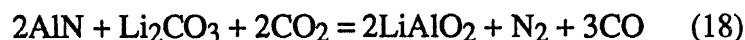
examined through a series of heat treatments at 600°C in flowing CO₂. The samples were infiltrated using the technique described previously, surfaces were cleaned to remove excess salt, and initial weight was measured. The samples were then heat treated for 100 hr intervals between which they were cooled to room temperature and re-weighed. The results of the exposure testing are shown in Figure 4.11.

The aluminum nitride samples exhibited an initial weight loss over the first 500 hours and then stabilized at a loss equivalent to ~15-20% of the initial salt content. In contrast, the lithium aluminate samples exhibited virtually no loss of weight for up to 2000 hr of exposure. Based on TGA results described in Section 4.1.3, the salt mixture itself was stable against vaporization under these conditions. Part of the observed weight losses may be due to reactions between the salt and the ceramic. This is supported by the X-ray phase analysis of the infiltrated samples before and after exposure for 2000 hr as shown in Table 4.15.

Table 4.15. Phase Analysis of Long-term Salt Retention Samples

Substrate	Initial Phases	Phases after 2000 hr
AlN	AlN, salts	AlN, LiAlO ₂ , salts
Lithium Aluminate	LiAl ₅ O ₈ , salts	LiAlO ₂ , LiAl ₅ O ₈ , salts
Lithium Aluminate	LiAlO ₂ , salts	LiAlO ₂ , salts

As can be seen in Table 4.15, both the aluminum nitride and the LiAl₅O₈ phase of lithium aluminate show some degree of reaction with the Li₂CO₃ portion of the alkali carbonate melt. Possible reactions to explain these results are:



These results indicate that there could be some long term stability questions for the use of aluminum nitride as a membrane support; however, since the weight loss stabilized after ~500 hr, it is likely that reaction (18) resulted in the formation of a passivating layer of LiAlO₂ on the surface of the AlN. The results in Table 4.15 also indicate the desirability of starting with phase pure LiAlO₂ as the substrate in the case of lithium aluminate. The lithium aluminate fabrication processes were directed to that end. The details of the LiAlO₂ development effort can be found in the report from GTC which is appended.

4.2.4 Ceramic Membrane Infiltration

A technique was developed to infiltrate the porous ceramic membranes with the molten carbonate salt mixtures. The process developed consisted of a vacuum infiltration technique in which the substrate was immersed in an excess of the salt powder, heated to a temperature greater than the anticipated test temperature under flowing CO₂, the furnace chamber was then repeatedly evacuated and back-filled with CO₂ to force the salt

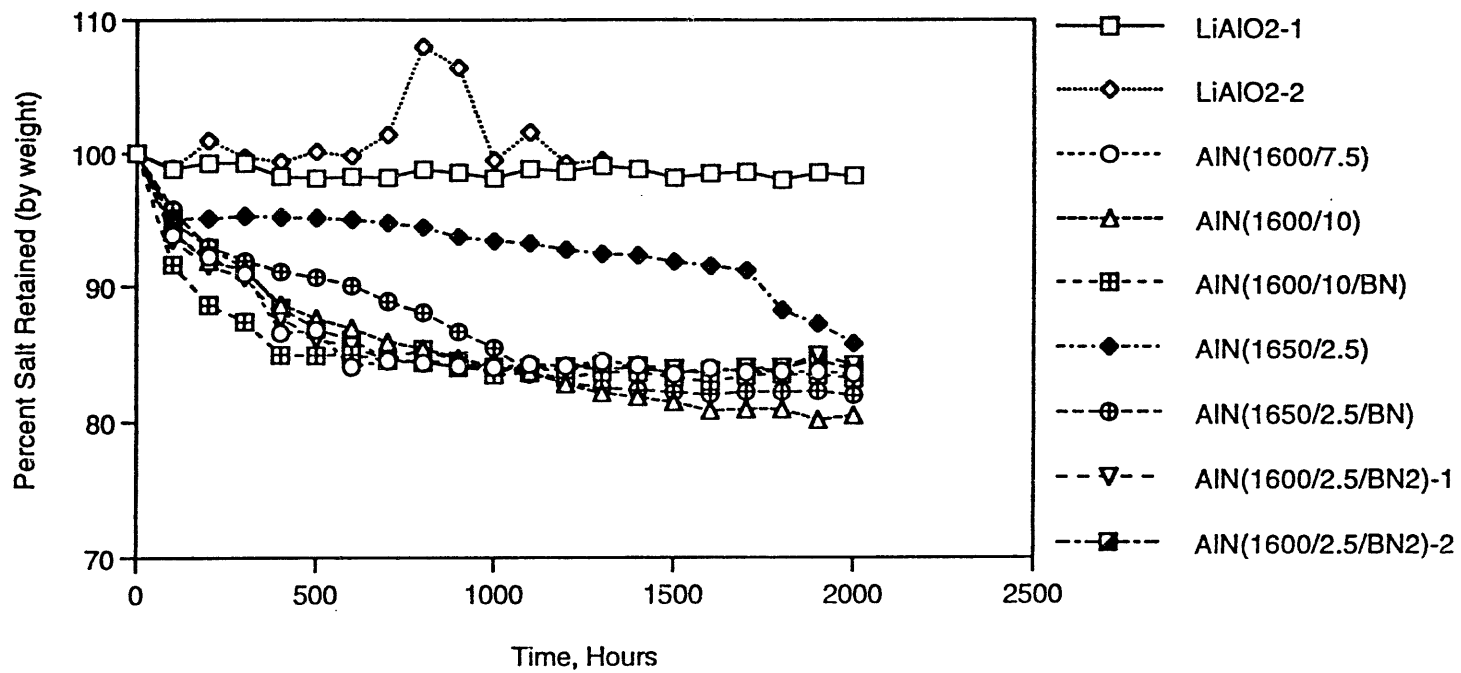


Figure 4.11 Long term salt retention of aluminum nitride and lithium aluminate porous samples

This page intentionally left blank.

Table 4.16. Planar Disc Support Infiltration Results

Sample #	Material	% Infiltrated	Sample #	Material	% Infiltrated
12496-13-1	AlN	80	12496-14-1	LiAlO ₂	65
12496-13-2	AlN	70	12496-14-2	LiAlO ₂	93
12496-13-3	AlN	82	12496-14-3	LiAlO ₂	97
12496-13-4	AlN	80	12496-14-4	LiAlO ₂	66
12496-15-1	AlN	83, cracked	12496-16-1	LiAlO ₂	80
12496-15-2	AlN	84	12496-16-2	LiAlO ₂	90
12496-15-3	AlN	77, cracked	12496-16-3	LiAlO ₂	100
12496-15-4	AlN	81	12496-16-4	LiAlO ₂	87
12496-17-1	AlN	83, cracked			
12496-17-4	AlN	88, cracked			
12496-17-5	AlN	83, cracked			
12496-17-6	AlN	76, cracked			
12496-17-7	AlN	78			
12496-18-1	AlN	68, cracked			
12496-18-2	AlN	69			
12496-18-3	AlN	61			
12496-19-3	AlN	62			
12496-19-4	AlN	63			
12496-20-2	AlN	66			
12496-21-1	AlN	66			
12496-21-2	AlN	72			
12496-21-3	AlN	68			
12496-21-4	AlN	75			
12496-21-5	AlN	72			
12496-21-6	AlN	73			
12496-23-1	AlN	76			
12496-23-2	AlN	65			
12496-23-5	AlN	68			
12496-23-6	AlN	72			
12496-23-7	AlN	74			
12496-23-8	AlN	67			
12496-24-1	AlN, thin	69			
12496-24-3	AlN, thick	34			
12496-24-4	AlN, thick	40			
12496-24-5	AlN	65			
12496-24-6	AlN	66			
12496-24-7	AlN	67			
12496-24-8	AlN	63			
12496-24-9	AlN	64			
12496-24-10	AlN	64			

Table 4.17. Tubular Support Infiltration Results

Sample #	Material	% Infiltrated
12496-25-T1	AlN Tube	80
12496-25-T2	AlN Tube	74
12496-25-T3	AlN Tube	82
12496-25-T4	AlN Tube	83

4.3 Membrane Testing

To evaluate membranes at high temperatures and pressures, a membrane test unit was constructed which is shown schematically in Figure 3.1. This unit was used in conjunction with the gas delivery system described in more detail previously (Section 4.1.3). Details of the membrane test unit and its operation can be found in Section 3.3. A brief description follows.

The membrane to be tested was sealed in a high temperature and pressure membrane cell constructed of stainless steel. The cell and membrane were heated to the required temperature in a furnace, usually 560°C. Gas lines from the mixing vessels carried gases across the two surfaces of the membrane. The feed gas mixture contained H₂S and other IGCC gases. The sweep gas consisted of H₂O and CO₂ in an inert gas. Gases from the feed which permeated the membrane were collected by the sweep gas and were analyzed by GC. The membranes examined consisted of the base composition carbonate mixture 30-A supported in a gold frit or a planar or tubular ceramic support.

Although the concept of a facilitated transport membrane for removal of H₂S at high temperatures is straightforward, a demonstration of its practicality is not. Numerous very significant problems were encountered during this effort, the most troublesome being H₂S-metal reactivity and the inability to obtain defect-free membranes. H₂S-metal reactivity is troublesome but solvable by methods discussed below. Defect-free membranes present a major challenge since, as described below, molten carbonate membranes are barriers to gases other than H₂S; defects permit permeation of relatively large quantities of these gases and an effective removal of H₂S is not obtained.

The concept of separation of H₂S from an IGCC gas mixture is illustrated in Figure 1.2. (p. 5) A feed gas mixture consisting of H₂S, CO₂, H₂ and other IGCC gases is passed across one surface of the membrane. From the feed side, the membrane can be viewed largely as a barrier to all gases except H₂S. These gases have relatively low physical solubilities in molten carbonates and, hence, relatively low permeabilities are expected. In contrast, the "solubility" of H₂S in the membrane is relatively high arising from its chemical reaction with the carbonate melt (reaction (1)). The sulfide formed at the feed interface diffuses across the membrane to the permeate side. There a sweep gas containing CO₂ and H₂O drives reaction (1) to the left reforming H₂S which is liberated into the sweep gas.

Estimates of the permeabilities of gases other than H₂S can be obtained from literature solubility and diffusivity data. For such gases which permeate by a solution-diffusion mechanism, P₀ is given by the equation (20) where S is the solubility and D is the diffusivity of a gas in the membrane medium, the molten carbonate mixture in the present case.

$$P_0 = S \cdot D \quad (20)$$

Literature data for H₂, CO, and CO₂ in molten carbonates were obtained from Selman and Maru.²³ Solubilities were calculated using an expression of the form $S = Ae^{-E/RT}$ for a ternary carbonate mixture at 560°C. Although the temperature of interest is outside the temperature range of the expressions for CO and CO₂, the errors are probably not large. Listed in Table 4.18 are calculated solubilities in units of mol(gas)/cc(melt)•atm and cc(g)/cc(melt)•cmHg. Estimates of diffusivities are less reliable. Experimental values for the D(H₂), e.g. 62x10⁻⁵ cm²/s at 560°C, are probably too large.²³ Alternatively, diffusivities can be calculated using the Wilke-Chang equation and values are available at 600°C for CO, CO₂, and H₂.²³ For the calculation of P₀, it was assumed that diffusivities at 600°C and 560°C were the same.

Table 4.18. Calculated permeabilities of CO, CO₂, and H₂ in a molten carbonate membrane.

Gas	S(mol/cc•atm) 560°C	S(cc/cc•cmHg) 560°C	D(cm ² /s) 600°C	P ₀ (Barrers)
CO	1.70x10 ⁻⁶	5.01x10 ⁻⁴	0.70x10 ⁻⁵	35
CO ₂	1.19x10 ⁻⁵	3.51x10 ⁻³	0.66x10 ⁻⁵	232
H ₂	6.29x10 ⁻⁶	1.85x10 ⁻³	1.12x10 ⁻⁶	210

4.3.1. Molten carbonate/gold frit membranes

Prior to availability of microporous ceramic supports, membranes consisting of molten carbonate salt mixtures immobilized in porous gold fritted discs were evaluated. In preliminary work, it was shown that a membrane consisting of molten mixture 30-A immobilized in a stainless steel fritted disc with 0.5 μm diameter pores could support a 40 psi pressure differential. Thus, gold frits with pore diameters of 0.5 μm were utilized initially. Two such membranes were evaluated at a temperature of 550°C and results are listed in Table 4.19. For both membranes, only H₂ was detected in the permeate when comparable feed and sweep pressures were used. H₂ permeabilities were 1600 and 3400 Barrers. These values are large compared with the theoretical H₂ permeability of 210 Barrers for a molten carbonate membrane (see Table 4.18), implying that the membranes have defects in the molten layer or that the molten layer was thinner than believed. For both membranes, increasing the feed pressure above those reported in Table 4.19 resulted in salt blow-through as indicated by the detection of large quantities of permeating gases. For membrane 11818-47-2, large amounts of CH₄ and H₂ along with some CO were detected in the sweep gas. This coupled with the observation of carbon powder deposits,

as confirmed EDS, in the membrane cell following the run, are consistent with reaction of CO₂ and H₂, possibly by the reactions listed below.



For membrane 11818-54-2, increased feed pressure resulted in detection of large quantities of H₂S, CH₄, COS, CO, and H₂ in the sweep. When examined at the end of the run, a rather large quantity of a yellow, metallic-appearing solid was found on the inner surface of the membrane holder. An analysis of this solid by EDS showed that it contained the elements Fe, Ni, and S. Clearly, the membrane cell and/or the gas lines leading to the cell had reacted with H₂S to yield nickel and iron sulfides.

The transmembrane pressure, ΔP, withstood by the above membranes, is far lower than that predicted for a molten carbonate salt/ceramic membrane by equation (17). For a pore of diameter 0.5 μm and an experimental contact angle of 52° for mixture 30-A, ΔP from equation (17) is 161 psi. Perhaps, some plugging of gas lines by carbon or metal sulfide led to an increase in pressure beyond this limit.

Table 4.19. Permselective properties of molten carbonate/gold frit membranes at 560°C.

Membrane	conditions (see below)	Feed P (psia)	Sweep P (psia)	gas	ppm in permeate	P _o (Barrers)
11818-47-2	a	29.1	22.2	H ₂	120	1600
				CO ₂	nd	-
				CH ₄	nd	-
11818-54-2	b	15.0	15.0	H ₂	130	3400
				H ₂ S	nd	
				CO ₂	nd	
				CH ₄	nd	

Conditions: a. Feed: 32.1% CO₂ and 21.4% CH₄ in H₂; sweep: 50.8% CO₂ in N₂.; feed and sweep flows: 30 sccm, 40 sccm.

b. Feed: 5.5% H₂S, 32.4% CO₂, and 16.2% CH₄ in H₂.; sweep: 50.8% CO₂ in N₂.; feed and sweep flows: 30 sccm, 40 sccm.

4.3.2. Planar molten carbonate/ceramic membranes

With the availability of a microporous ceramic, attention was shifted to examination of membranes consisting of the molten base carbonate composition 30-A immobilized in planar microporous ceramic support consisting of AlN or LiAlO₂. A summary listing of the membranes tested is provided in Table 4.20.

4.3.2.1. Membrane Sealing. Sealing of AlN/salt membranes in the membrane cell often proved to be difficult. Many membranes cracked upon sealing. It was found that the use of a sealing C-ring in place of an O-ring resulted in membranes which were more often crack-free. Somewhat later it was found that elimination of the C-ring and sealing using a graphite tape proved to be more reliable. See Section 3.3 for details.

4.3.2.2 Testing with H₂S containing feeds. The most significant problem associated with testing of molten salt/ceramic membranes was the reactivity of H₂S with the metal of the membrane holder and cell. This is illustrated by the results for a molten carbonate/AlN membrane (12334-92-1) evaluated at a membrane temperature of 560°C. Using humidified feed (2% H₂S, 2% CO₂, 10% CH₄, 26% H₂ in N₂) and sweep gases (10% CO₂ in N₂), no permeating gases were detected in the sweep during the first hour of operation. In addition, feed and sweep pressures were independent of one other. These observations are consistent with a membrane which was largely defect free under the experimental conditions. Subsequently, relatively large quantities of CH₄, H₂ and CO were detected in the sweep suggestive of formation of defects in the molten salt layer.

Table 4.20. Listing of molten carbonate/ceramic planar membranes tested.

Membrane	Support	Comments
12334-92-1	AlN	Membrane cracked
12334-91	AlN	Withstood brief ΔP of 70 psia; intact membrane; data in Table 4.16
12334-92-2	AlN	Membrane cracked
12344-92-4	AlN	Membrane cracked
12344-92-5	AlN	Operated briefly at 560°C before a hole developed; data in Table 4.19
12496-2-5	AlN	Membrane cracked.
12496-2-4	AlN	Membrane cracked
12496-2-2	AlN	Data in Table 4.23
12496-2-3	AlN	Data in Table 4.21
12496-2-1	AlN	Membrane cracked after initial data at ambient pressure
12496-2-6	AlN	Membrane cracked
12496-5-6	AlN	Membrane cracked after initial data at ambient pressure
12496-5-2	AlN	Membrane cracked
12496-5-1	AlN	Data in Table 4.21; cracked upon raising pressure above ambient
12496-11-2	LiAlO ₂	Large and variable concentrations of permeating gas due to failed flow controller
12496-11-1	LiAlO ₂	Pressure differential could not be maintained; cracked?
12496-14-3	LiAlO ₂	Data in Table 4.23; unrealistically large CO ₂ P _O ; cracked at higher feed pressures.
12496-15-4	AlN	Data in table 4.23
12832-15-2	AlN	Data in Table 4.24
12496-16-3	LiAlO ₂	Data in Table 4.24
12496-16-4	LiAlO ₂	Data in Table 4.24
12496-18-2	AlN	Data in Table 4.24
12496-18-3	AlN	Data in Table 4.24
12496-17-7	AlN	Data in Table 4.24
12496-19-4	AlN	Data in Table 4.24

Almost no H₂S was detected in the sweep probably due to reaction of H₂S with the Inconel membrane cell. Upon examination after the run, the membrane was found to have cracked. In addition, relatively large amounts of black, gray, and gold colored solids were observed throughout the cell. Some of these deposits resulted in blockage of gas lines. This evidently led to a plugging of the gas line which may have resulted in cracking of the membrane. EDS analysis of the various deposits indicated the presence of the following elements: O, S, K, Ca, Cr, Fe, Ni. The presence of K, Ca, O can be ascribed to the carbonate mixture while S, Cr, Fe, and Ni are the result of metal sulfide formation from reaction of H₂S with the Inconel membrane cell.

Somewhat less metal-H₂S reactivity was observed when the molten salt/AlN membrane 12334-91 was evaluated using dry feed (H₂S, CO₂ in N₂) and sweep (CO₂ in N₂) gases and a stainless steel 304-membrane cell. Results are listed in Table 4.21. Feed and sweep back pressures were adjusted to keep the transmembrane pressure (ΔP), relatively small, approximately 5 psia. However, during adjustment to reach the final set of pressures, a ΔP of about 70 psi occurred but the membrane apparently suffered no cracking or salt blow-through as implied by the relatively small concentration of permeating gases. As listed in Table 4.14, the calculated ΔP for a AlN membrane with 1 μm pores is 65 psi. Since water was absent from the sweep gas, facilitated transport of H₂S was not expected. At the feed pressure examined, 26.8 psia, no H₂S was detected in the permeate but at two higher pressures, H₂S permeabilities of 10,900 and 2,270 Barrers were obtained. However, it is clear that reaction of H₂S with the metal membrane cell had occurred. At all three feed pressures, significant quantities of H₂ and CO were observed in the permeate. H₂ is a result of an H₂S/metal reaction as in reaction (14) and CO arises from a subsequent reaction of H₂ and CO₂ (reaction (13)).

It was clear that obtaining meaningful H₂S permeation data at the low flows and elevated temperature using stainless steel components, and at relatively low gas flow rates, would be virtually hopeless. Since the absolute quantity of H₂S permeating the relatively thick salt/ceramic membranes was small, loss of H₂S due to reactivity with metal had a major impact on the H₂S permeabilities obtained. Although materials which are inert with respect to H₂S are available (see later), construction and testing of membrane cells composed of these would have required a long time. A shorter term alternative was to render inert the metal surface exposed to H₂S. Two possible techniques considered were gold plating and alonizing. Alonizing gave a membrane cell with fairly rough surfaces which prevented successful sealing of membranes in the cell. Gold plating, of course, gave smooth surfaces; therefore, membranes could be successfully sealed in the cell making it possible to evaluate the membranes.

Table 4.21. Permselective properties of molten carbonate/ceramic membranes at 560°C using H₂S containing feeds.

Support	Membrane	Conditions (see below)	Feed P (psia)	Sweep P (psia)	gas	ppm in permeate	P _O (Barrers)
AlN	12334-91	a	26.8	20.1	H ₂ S	nd	-
					H ₂	187	-
					CO	406	-
		a	46.4	48.4	COS	nd	-
					H ₂ S	162	10,900
					H ₂	26	-
					CO	268	-
					COS	22	-
					H ₂ S	151	2270
a	207.3	204.0	H ₂	13	-		
			CO	670	-		
			COS	181	-		
			H ₂ S	nd	-		
AlN	12496-5-1	b	15.0	15.0	H ₂ S	nd	-
					CO	3800	149,000
					COS	nd	-
					H ₂	2700	181,000
AlN	12496-2-3	c	16.6	16.5	CO	9000	-
					H ₂	793	-
					H ₂ S	nd	-

Test conditions:

- Feed: 6.1% H₂S, 5.7% CO₂ in N₂; sweep: 11.3% CO₂ in N₂; both dry; flow rates, 50 sccm.
- Feed: 0.62% H₂S, 5.52% CO₂, 15.84% CO, 9.52% H₂ in N₂ or 0.59% H₂S, 5.64% CO₂, 16.10% CO, 9.43% H₂ in N₂; sweep: 20% CO₂ in N₂; both humidified by passage through 60°C water bubblers; flow rate, 25 sccm.
- Feed: 10% CO₂, 10% H₂S in N₂; sweep: 20% CO₂ in N₂; both gases through 60°C water bubblers at 25 sccm.

The molten carbonate/AlN membrane 12496-2-3 in a gold plated holder was evaluated at 560°C using feed (10% H₂S and 10% CO₂ in N₂) and sweep (20% CO₂ in N₂) gases humidified by passage through water bubblers at 60°C. As indicated in Table 4.21, no H₂S was detected in the sweep but 9000 ppm CO, 800 ppm H₂ and a trace of COS were. These results imply H₂ formation by reaction of H₂S with metal. In fact, examination of the cell upon completion of the run revealed solid deposits on the sealing C-ring surfaces, the feed and sweep side flanges and on the membrane surface. Two visually different deposits were observed on the sweep side flange and on the AlN surface. Elemental compositions of these deposits were determined by EDS and are listed below in Table 4.22.

Table 4.22. Elements present as determined by EDS in the membrane cell after evaluation of membrane 12496-2-3.

Location	elements present
feed side flange	O, S, K, Si, Cr, Fe, Ni
sweep side flange	1. O, S, K, Fe, Ni 2. O, S, K, Ca
AlN surface	1. Black - O, S, K., Al 2. Gold - K, Au
C-ring feed side	O, S, K, Si, Ti, Cr, Fe, Ni

Presumably, the elements S, Si, Ti, Cr, Fe, and Ni arise from reaction of the base metal of the membrane cell or the tubing with H₂S while O, K, and Ca are from the carbonate mixture. These results clearly indicate that gold plating was unsuccessful in producing an H₂S-inert surface, at least at the relatively low flow rates, 25 sccm, used in these experiments.

Two additional membranes were examined using gold plated membrane cells. For one of these (molten salt/LiAlO₂ membrane 12496-11-2), equipment failure prohibited collection of permselective data but solid deposits like those described above were observed. The molten carbonate/AlN membrane 12496-5-1 exhibited no detectable permeation of H₂S; however, very high permeabilities of CO and H₂ were observed when a feed containing H₂S, CO₂, CO and H₂ was used. This indicates substantial reactivity of H₂S with metal and some defects in the membrane. A slight increase in the feed pressure resulted in cracking of the membrane.

A gold plated membrane cell in the absence of a membrane was examined to insure that the membrane was not responsible for decomposition of H₂S. The sweep side of a holder was sealed off so that gas could exit only through the feed reject, which was analyzed by GC. Data was collected at 560°C using feeds containing about 11 to 0.4% H₂S in N₂ and for a feed containing about 0.5% H₂S and 5% H₂ in N₂. Average or final concentrations of H₂S and H₂ in the feed reject are listed in Table 4.23.

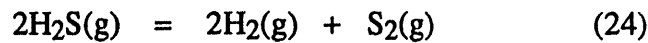
Table 4.23. Analysis of H₂S gas mixtures passed through a gold plated membrane cell at 560°C.

Feed #	Feed composition, %		gas conc., % in feed reject		% H ₂ S decomposition	value of K (see equation 25 below)
	H ₂ S	H ₂	H ₂ S	H ₂		
1	10.98	-	10.93	0.200	0.6	3.3x10 ⁻⁷
2	5.18	-	5.11	0.116	1.4	3.0x10 ⁻⁷
3	2.72	-	2.62	0.0794	3.7	3.7x10 ⁻⁷
4	0.428	-	0.395	0.0412	7.7	2.3x10 ⁻⁶
5	0.526	4.92	0.451	4.96	14.3	4.7x10 ⁻²

For each of the above feeds, some H₂S decomposed upon passage through the membrane holder. Except for feed number 1, the amount of H₂S consumed and H₂ generated were comparable. The percent decomposition of H₂S based on the initial concentration of H₂S and that in the feed reject are listed above.

One possible fate of H₂S upon passage through a hot membrane cell is thermal decomposition as in reaction (24) below. Thermal decomposition of H₂S at elevated temperatures is well known and, in fact, has been proposed as a method to dispose of H₂S or to produce H₂.^{25,26} Various catalysts have been evaluated in an attempt to make decomposition of H₂S practical.²⁷ In addition, composite-platinum membranes have recently been used to promote thermal decomposition of H₂S by permeation of product H₂.²⁸

Using a simple free energy calculation,¹³ ΔG° for reaction (24) at 527°C is 24.4 kcal/mole or K = 2.1x10⁻⁷.



$$K = \frac{[\text{H}_2]^2 \cdot [\text{S}_2]}{[\text{H}_2\text{S}]^2} \quad (25)$$

Values of the above equilibrium constant expression were calculated for feeds 1-4 by assuming that the S₂ concentration was one half that of the H₂ concentration. For feed 5, the concentration of S₂ was assumed to be one half of the H₂S consumed. The calculated values of K are each greater than that expected for simple thermal decomposition of H₂S and implies an additional source of H₂S decomposition and H₂ production. This is particularly apparent at low feed concentrations of H₂S (feeds 4 and 5). In addition, the presence of H₂ in feed 5 should suppress thermal decomposition of H₂S. Decomposition of only 9x10⁻⁵% H₂S or 0.005 ppm is expected for the initial concentrations of feed 5 listed in Table 4.23, significantly lower than the observed value of 14.7%. The above data is consistent with two modes of H₂S decomposition: (1) thermal (2) reaction with metal. For feeds with relatively high H₂S concentrations, thermal decomposition predominates. At lower feed concentrations, proportionally less thermal decomposition occurs and decomposition by reaction with metal becomes more apparent.

It is worth noting that extended exposure of a gold plated membrane cell to H₂S containing feeds at elevated temperatures resulted in the deposition of a dull, crystal-like layer on the gold surface. The elemental composition by EDS (S, Cr, Mn, Fe, Ni, Cu, Zn, and Au) confirmed the presence of metal sulfides. This layer may result in some passivation with respect to H₂S. Exposure of the gold plated cell to H₂S containing feeds for an extended time at 560°C resulted in a decrease in H₂S decomposition from 37% initially to about 2.3% after seven days.

4.3.2.3 Testing with non-H₂S containing feeds. As a result of H₂S-metal reactivity, molten salt/ceramic membranes were evaluated using feeds which contained no H₂S. Results for the various membranes examined are listed in Table 4.24. For these membranes, the feed compositions, which were determined at ambient temperature, were assumed to be unchanged by heating to a membrane temperature of 560°C. This is not, of course, the case when H₂ and CO₂ are present in the feed since CO was observed in the permeate of these membranes. Nonetheless, the permselective data reported in Table 4.24 is at least qualitatively useful. For example, membrane 12344-92-5 exhibited very large CO₂ and H₂ permeabilities. Such results are typical of a membrane with holes or defects which permit Knudsen flow of gases but which are small enough to maintain a transmembrane pressure of greater than 20 psia. Substantial quantities of CO were observed in the permeate even though none was present in the feed. It presumably resulted from reaction of CO₂ and H₂ (reaction (13)).

Complications associated with the presence of both CO₂ and H₂ at elevated temperatures were eliminated by using feeds consisting only of CO₂ and an inert gas. Using such feeds, a series of membranes were examined. Some resulted in very large permeabilities of CO₂ and the inert gas, suggestive of holes or defects in these membranes (12496-14-3, 12495-15-4). Others gave lower permeabilities due to lower defect rates. However, the CO₂ permeabilities of none of these membranes were comparable to the theoretical CO₂ permeability of a molten carbonate membrane, 232 Barrers, (see Table 4.18). For some membranes (e.g. 12496-2-2), significant amounts of CO were detected in the sweep, even when only CO₂ and an inert gas were present in the feed. Apparently the membrane and/or the membrane cell provide reactive surfaces at which reduction of CO₂ occurs.

For membrane 12496-2-2, using a CO₂/Ar feed and initial feed and sweep pressures of 37.8 psia and 20.0 psia, a large quantity of CO₂ was detected in the sweep. This is suggestive of pinholes or other defects in the membrane. However, over the period of several hours these defects apparently sealed and the data listed in Table 4.24 was obtained.

As mentioned previously, an alternative membrane sealing technique using graphite tape in place of the gold C-rings proved to be more successful. In general, it appeared that the use of graphite tape resulted in fewer cracked membranes. The permselective properties of membranes sealed using this technique and using non-H₂S containing feeds are listed in Table 4.25. For one such membrane, the molten carbonate/LiAlO₂ membrane 12496-16-3, a bench top pressure check was performed at room temperature using 20 psia. No gas flow across the membrane was detected. Membranes examined using dry feed and sweep gases exhibited CO₂ permeances in the range of about 1,200 to 10,000 Barrers. In each case, permeabilities of the inert gases N₂ or Ar were greater than that of CO₂. Visual examination of the above membranes revealed no evidence of cracking or other defects, but there appears to have been some migration of salt in the AlN membranes.

Table 4.24. Permselective properties of molten salt/ceramic membranes at 560°C using non-H₂S containing feeds.

Support	Membrane*	Conditions (see below)	Feed P (psia)	Sweep P (psia)	gas	ppm in permeate	P _o (Barrers)
AlN	12344-92-5	a	18.9	20.4	CO ₂	1397	38,000
					H ₂	25599	834,000
					CO	14225	-
			35.8	27.8	CO ₂	55903	906,000
					H ₂	58113	1,060,000
					CO	39972	-
			58.6	31.7	CO ₂	116230	1,220,000
					H ₂	97091	1,110,000
					CO	82888	-
LiAlO ₂	12496-14-3	d	15.0	15.0	CO ₂	5922	234,000
					N ₂	15431	131,000
AlN	12496-15-4	d	16.0	15.6	CO ₂	801	19,000
					N ₂	2189	17,400
AlN	12496-2-2	b	20.4	15.7	CO ₂	1772	6,640
					Ar	**	-
					CO	453	-
		41.0	15.9	CO ₂	3104	5760	
				Ar	**	-	
				CO	428	-	

Test conditions

- a. feed: 37.1% CO₂, 33.6% H₂ in N₂; N₂ sweep; both gases passed through 60°C water bubblers; flow rates 50 sccm.
- b. Feed: 50.0% CO₂ in Ar; He sweep; both dry, flow rates 10 sccm unknown sources were also detected in the permeate.
- d. Feed: 25.3% CO₂ in N₂; sweep: helium; both dry; 25 sccm sweep flow.

Notes:

- * all membranes sealed in membrane cell using a C-ring.
- ** Ar detected but not quantified.

Table 4.25. Permselective properties of molten carbonate/ceramic membranes at 560°C using non-H₂S containing feeds. Dry feed and sweep gases unless stated otherwise.

Support	Membrane***	Conditions (see below)	Feed P (psia)	Sweep P (psia)	gas	ppm in permeate	P _o (Barrers)
AlN	12832-15-2	a	16.5	15.1	CO ₂	344	9740
					Ar	**	-
LiAlO ₂	12496-16-3	a	16.4	15.5	CO ₂	199	5670
					Ar	trace**	-
AlN	12496-19-4	b	53.3	15.5	CO ₂	213	5290
					CO	24	1200
					N ₂	554	9200
		b-wet	59.2	15.7	CO ₂	507	11300
					CO	116	5130
					N ₂	634	9480
AlN	12496-17-7	c	54.3	15.5	CO ₂	87	3480
					Ar	216	2020
		c-wet	52.1	15.5	CO ₂	7685	320,000
					Ar	29,925	292,000
		d	55.6	15.3	CO ₂	17,412	386,000
					CO	7,604	328,000
					He	**	-
AlN	12496-18-3	e	37.7	15.5	CO ₂	187	9570
					Ar	802	12400
		e	44.9	15.5	CO ₂	39	1670
					Ar	344	3040
		e	62.4	15.5	CO ₂	62	1900
					CO	71	-
					Ar	441	4050
LiAlO ₂	12496-16-4	f	16.5	15.5	CO ₂	58	6190
					Ar	491	14400
		g	49.0	15.5	CO ₂	11	*
					Ar	199	*
AlN	12496-18-2	h	41.4	15.5	CO ₂	12	1400
					Ar	182	5450
		i	64.5	15.5	CO ₂	9	1190
					Ar	208	7070

Test conditions: dry = dry feed and sweep; wet = feed and sweep gases passed through 60°C water bubblers.

- a. feed: 20.5% CO₂ in Ar; sweep: N₂; both dry. Small quantities of CH₄ and H₂ in sweep.
- b. feed: 31.0% CO₂, 15.7% CO in N₂; sweep, helium; feed flow 112 sccm, sweep flow 109 sccm.
- c. feed: 9.0% CO₂ in Ar; sweep, helium; feed flow 112 sccm, sweep flow 109 sccm.
- d. feed: 33.4% CO₂, 17.2% CO in He; sweep, N₂; feed flow, 112 sccm; sweep flow, 109 sccm.
- e. feed: 23.2% CO₂ in Ar; sweep, helium; feed flow, 120 sccm; sweep flow, 118 sccm
- f. feed - 21.8% CO₂ in Ar; feed flow rate 100 sccm; sweep flow rate, 101 sccm.
- g. same as f but sweep flow rate undetermined.
- h. feed: 20.4% CO₂ in Ar; feed and sweep flow rates, 260 sccm.
- i. feed: 20.4% CO₂ in Ar; feed and sweep flow rates, 460 sccm.

Notes: *permeability could not be calculated since sweep flow rate was not determined; **helium detected but not quantified; ***all membranes sealed in cell using graphite tape.

The effect of the feed pressure of CO₂ on its permeability was evaluated for two different membranes. For membrane 12496-18-2, CO₂ permeabilities were roughly the same at the two different pressures evaluated. This is consistent with permeation of CO₂ by a solution-diffusion mechanism, as is expected. Membrane 12496-18-3 was examined using a CO₂/Ar feed at three different feed pressures. At the lowest pressure examined, the CO₂ permeability was the largest which might suggest facilitated transport of CO₂. However, the permeability of N₂ was also large compared to values at higher pressures. A more reasonable explanation is that small defects were present initially which subsequently sealed.

Humidification of feed and sweep gases apparently has a substantial effect on gas permeabilities. For example, the CO₂ permeabilities of membrane 12496-17-7 increased 100-fold upon humidification of feed and sweep gases. Such large permeabilities are suggestive of defects in the membrane. Upon returning to dry gases, CO₂ and other permeabilities remained large. The effect of gas stream humidification on the performance of membrane 12496-19-4 was quite different. Humidification resulted in an approximate doubling of the CO₂ permeability and a four-fold increase in the CO permeability, but the N₂ permeability was unchanged.

4.3.3 Alternative materials of construction for membrane cells

Although the time involved in fabrication and testing of membrane cells consisting of materials other than stainless steel or related metals would likely be quite long, some preliminary investigations of alternative materials were pursued. Two such materials were quartz and alumina. The reactivity of H₂S with these materials was evaluated by passing a stream of approximately 6% H₂S in N₂ at 25 sccm through tubes of either material. The exit stream was analyzed by GC and data for various temperatures are listed in Table 4.26.

Table 4.26. Analysis of 6% H₂S in N₂ feed after passage through quartz or alumina tubes at the indicated temperatures.

Material	T(°C)	gas conc (ppm)	
		H ₂ S	H ₂
Quartz	23	61840	nd
	560	63660	nd
	600	64530	23
	650	63650	60
	700	63450	203
Alumina	23	60010	nd
	500	60680	nd
	550	61070	nd
	600	60190	nd
	650	61180	nd
	700	61650	12

In addition, small quantities of CO₂, 50-60 ppm, were detected in the exit from the quartz tube at 560-700°C. It is presumed that this corresponds to a slight leakage at the sealing gasket. No CO₂ was detected in the exit from the alumina tube. It would appear that both quartz and alumina are essentially inert with respect to H₂S at flow rates comparable to those used in membrane experiments. Hence, either material could be used to fabricate an H₂S-inert membrane cell.

4.3.4 Planar and tubular molten carbonate/ceramic membranes. Testing at Research Triangle Institute.

A series of membranes consisting of the molten base composition mixture 30-A immobilized in planar or tubular microporous ceramic supports were evaluated at Research Triangle Institute (RTI). Through the use of fairly high flow rates of gases, liters per minute rather than milliliters per minute, much of the difficulties associated with H₂S-metal reactivity were minimized. The permselective properties of the membranes tested by RTI are detailed in a separate report which is in the Appendix.

4.3.5 Modeling of membrane performance

A model designated CMEM was developed which predicts the permselective properties of a molten carbonate membrane. The model is also useful for testing the effect of any of a number of physical parameters that affect membrane performance. The most important of which are the equilibrium constant of the facilitating reaction (reaction (1)) and the sweep and feed stream pressures and compositions. The central premise of the model is that only H₂S is solubilized in the membrane by reaction with the carbonate melt as in reaction (1). Other gases, including H₂S, permeate the membrane by physically dissolving as discrete molecules and diffusing. The model was designed to evaluate membranes in a counterflow configuration.

If it is assumed that the chemical equilibrium between H₂S and the melt as in reaction (1) exist, and without specifying or having knowledge of the forward or reverse rates of reaction, the assumption must be made that the reaction occurs only at the gas-membrane interface. The additional assumption that mass transfer resistance in the gas phase is negligible means that the partial pressures of H₂S, CO₂, and H₂O at the membrane interface can be set equal to the gas stream partial pressures. If the only anions present in the melt are sulfide and carbonate, the concentration of sulfide ion is given by:

$$[S^{2-}] = \frac{C_T K_1 P_{H_2S}}{P_{H_2O} P_{CO_2} + K_1 P_{H_2S}} \quad (26)$$

where C_T is the sum of the concentration of S²⁻ and CO₃²⁻ ions at equilibrium. The flux of H₂S across the membrane is taken to be equal to the flux of sulfide ion following Fickian diffusion:

$$\text{Flux}_{\text{H}_2\text{S}} = \frac{D_{\text{S}^{2-}}}{\delta} ([\text{S}^{2-}]_1 - [\text{S}^{2-}]_2) \quad (27)$$

where δ is the thickness of the membrane, $D_{\text{S}^{2-}}$ is the diffusivity of the sulfide ion, and $[\text{S}^{2-}]$ is the concentration of sulfide ion on the feed ($i=1$) or sweep ($i=2$) side of the membrane. By the stoichiometry of reaction (1), the fluxes of CO_2 and H_2O are equal to that of H_2S but permeate from the sweep to feed side of the membrane rather than from feed to sweep as for H_2S . Transport of H_2O and CO_2 are assumed to occur by the reaction mechanism alone and transport by solution/diffusion is neglected. For the "inert" gases such as H_2 and CO , transport by a solution-diffusion mechanism was presumed. The flux of these gases was obtained from an expression analogous to equation (27) but where concentrations were those of physically dissolved gases at the feed and sweep interfaces.

The input required to run the program included the diffusivity and solubility of each inert gas, the diffusivity of the sulfide ion, and the equilibrium constant, K_1 . Each of these is sensitive to temperature and composition of the molten salt mixture. CMEM will prompt for the diffusivity and solubility of each inert beginning with N_2 . Given a value for N_2 diffusivity, CMEM provides an estimate for the diffusivity of the remaining inert gases based on the Wilke-Chang equation and tabulated molar volumes (cc/gmole).²³ The diffusivity of the sulfide ion may be estimated from the value for sodium ion. The diffusivity of S^{2-} is typically about 0.3 times that of Na^+ , based on ionic volumes.²³

CMEM also requires the molten salt anion concentration, C_T , and the membrane thickness, δ . The anion concentration is the liquid density divided by the average molecular weight of salt species present. The membrane thickness is the actual thickness of the molten salt barrier unless a tortuosity factor is required for a given porous support. Since experimental tortuosities were not determined, no tortuosity corrections were applied.

Process parameters required by CMEM are the ratio of sweep to feed flow rates, feed and sweep compositions, and the total pressure of each stream. The pressure drop from module inlet to outlet on either side of the membrane is assumed to be negligible. A target concentration of H_2S in the clean outlet stream (feed reject) is required.

Input and output for a run of CMEM are illustrated in Table 4.27. The input file lists the information required to run the program. The composition of the feed and sweep streams, as mole fractions, are specified in lines 3 and 5 in the following order: H_2S , H_2O , CO_2 , N_2 , CO , H_2 , NH_3 , and CH_4 . Line 7 is the mole fraction of H_2S in the feed reject. Membrane thickness in cm is listed in line 8. Other parameters are self explanatory.

Using the input parameters, CMEM first estimates the performance of a counter-flow module based on 'log-mean driving force' assumptions. These simplifications are well suited to streams dilute in the active gases, and permits an initial check as to whether

target outlet concentration of H₂S is achievable. A more rigorous calculation, involving an integration along the membrane surface and calculation of fluxes and gas phase compositions at each point, is then performed. An example of the results of such a calculation are listed in the output file in Table 4.27. Reported are the H₂S flux, the area required to achieve the target concentration of H₂S in the feed reject, H₂S permeance, selectivity, and fractional conversion to S²⁻ at the feed and sweep interfaces.

Table 4.27. Input and output data for the program CMEM.

Example Input File INPUT.PAR

```

1.0          | Specific Feed Rate must be 1.0
1.0          | Q2i, moles Sweep per mole Feed
0.5      1.0      5.0      | 48.0  21.0  20.0  0.30  4.20  | Y1i
20.0       | P Feed (atm)
0.0      5.0      10.0     | 80.0   5.0   0.0   0.0   0.0   | Y2i
15.0       | P Sweep (atm)
0.001      | Y H2S Reject
1.0        | delta (cm)
.20000E-03 .10000E-03 | Diff., Solub of N2 (cm*cm/sec and mmole/cc/atm)
.20000E-03 .20000E-02 | Diff., Solub of CO (cm*cm/sec and mmole/cc/atm)
.32000E-03 .50000E-02 | Diff., Solub of H2 (cm*cm/sec and mmole/cc/atm)
.22000E-03 .10000E-02 | Diff., Solub of NH3 (cm*cm/sec and mmole/cc/atm)
.21000E-03 .10000E-02 | Diff., Solub of CH4 (cm*cm/sec and mmole/cc/atm)
.30000E-05 | Diffusivity of Sulfide Ion (cm*cm/sec)
2.0        | Equilibrium Const K1 (atm)
20.0       | CO3 Anion Concentration (mmole/cc)

```

Example Output File OUTPUT.DAT

```

RUN NUMBER          1
-----
Module Performance:
Flux of H2S          0.14E-04 (mmoles/sec/cm^2)
Area required        0.28E+03 * Feed Rate (cm^2 open area)
                    (Feed Rate in mmoles/sec)
*Permeance of H2S   0.14E-03 (mmole/sec-sq.cm-atm)
                    0.46E-04 (scc/sec-sq.cm-cmHg)
*Selectivity H2S/Inerts 0.11E+03
Fractional Conv. to S--
- Feed Side          0.12E+00
- Sweep Side         0.91E-05
                    *Based on Feed/Sweep pressure drop

```
